Enhancing the Secrecy Performance of the Spatial Modulation Aided VLC Systems with Optical Jamming

Fasong Wang, Rui Li, Jiankang Zhang, Shijie Shi, Chaowen Liu

PII: S0165-1684(18)30399-2
DOI: https://doi.org/10.1016/j.sigpro.2018.12.008
Reference: SIGPRO 7003

To appear in: *Signal Processing*

Received date: 2 May 2018
Revised date: 14 November 2018
Accepted date: 12 December 2018

Please cite this article as: Fasong Wang, Rui Li, Jiankang Zhang, Shijie Shi, Chaowen Liu, Enhancing the Secrecy Performance of the Spatial Modulation Aided VLC Systems with Optical Jamming, *Signal Processing* (2018), doi: https://doi.org/10.1016/j.sigpro.2018.12.008

HIGHLIGHTS

- A friendly optical jamming aided secrecy enhancement scheme is designed for the proposed SM-VLC system.
- The secrecy performance of the SM-VLC system with optical jamming is analyzed, which includes the average mutual information (AMI), lower bound on AMI and its closed-form expression approximation and achievable secrecy rate.
- Closed-form approximations for the AMI of Alice-to-Bob and Alice-to-Eve are derived.
- The power allocation strategy for the proposed optical jamming based SM-VLC system is considered.
- The pairwise error probability and bit error rate (BER) of the proposed friendly optical jamming aided secrecy enhancement SM-VLC system are derived.

Enhancing the Secrecy Performance of the Spatial Modulation Aided VLC Systems with Optical Jamming

Fasong Wang, Rui Li, Jiankang Zhang, Shijie Shi, Chaowen Liu

Abstract

In order to enhance the secrecy performance of the spatial modulation (SM) aided visible light communication (VLC) system, an optical jamming aided secrecy enhancement scheme is proposed in this paper, in which transmitter (Alice) sends the optical jamming signals and the confidential signal simultaneously with amplitude and power constraints, wherein the truncated Gaussian distribution is adopted by the optical jamming signals for the considered constraints. Additionally, with finite discrete support set of the channel inputs' distribution, the corresponding secrecy performance is systematically analyzed for the optical jamming aided SM-VLC system, which includes the average mutual information (AMI), the lower bound on AMI and its closed-form expression approximation and the achievable secrecy rate. Furthermore, the power allocation problem for the proposed SM-VLC systems with optical jamming is considered. Finally, extensive simulation results are presented to validate our analytical results and the secrecy versus bit error ratio (BER) trade-off is characterized.

Index Terms

Visible light communication (VLC), spatial modulation (SM), physical layer security (PLS), optical jamming, achievable secrecy rate, power allocation.

F. Wang is with the School of Information Engineering, Zhengzhou University, Zhengzhou, 450001, Henan, China. (E-mail: iefswang@zzu.edu.cn)

R. Li is with the School of Science, Henan University of Technology, Zhengzhou, 450001, Henan, China. (E-mail: slxlr@haut.edu.cn)

J. Zhang is with the Southampton Wireless Group, School of Electronics and Computer Science, University of Southampton, Southampton SO17 1BJ, UK. (E-mail: jz09v@ecs.soton.ac.uk)

C. Liu is with the Ministry of Education Key Laboratory for Intelligent Networks and Network Security, Xi'an Jiaotong University, Xi'an, 710049, Shaanxi, China. (E-mail: liucwhb@gmail.com)

F. Wang would like to acknowledge the financial support of the NSFC under Grant 61401401, the China Postdoctoral Science Foundation Project under Grant 2015T80779 and the Young Teachers Special Research Foundation Project of Zhengzhou University under Grant 1521318001. J. Zhang would like to acknowledge the financial support of the NSFC under Grant 61571401 and the Innovative Talent of Colleges and University of Henan Province under Grant 18HASTIT021.

I. Introduction

A. Background

With the popularity of cloud computing and the development of Internet-of-Things (IoTs), there is an unprecedented requirement for wireless communication systems with massive connectivity, low latency, and diverse data rates. As a promising wireless transmission technique, visible light communication (VLC), which exploits the existing high brightness light-emitting diodes (LEDs) for both illumination and data communications [1], with its unique features such as immunity to electromagnetic interference, unlicensed spectrum, low cost, and the potential of spatial reuse of frequency bands in adjacent optical attocells, has gained considerable attention for several decades from both academia and industry [1]–[3]. However, being the broadcast nature of wireless transmissions, data transmissions over VLC downlinks are inherently vulnerable to be intercepted by unintended receivers or eavesdroppers, which are located at the illumination area of the source LEDs.

Therefore, information security becomes an urgent issue to be solved in VLC system, especially when the communicating nodes are explosed to public areas such as public train stations, offices and shopping malls, *et al*. [4]. In addition, securing VLC transmissions is also necessary when there exist non-light of sight (NLoS) reflections inside a room as well as partially covered windows, floor-to-door gaps and keyholes *et al*. [5], [6]. Traditional security schemes are performed at upper-layers of the wireless systems by using access control, password protection and end-to-end encryption [7], [8]. Nevertheless, these computational burden based security strategies may no longer hold with the development of quantum computers. As a complement or even an alternative to the conventional secrecy solutions, various physical layer security (PLS) techniques have been proposed recently to realize perfect security in wireless communication systems, which exploits the channel characteristics to hide information from eavesdroppers and does not rely on the upper-layer encryption [9]–[12]. These works focused on maximizing the secrecy capacity of a wiretap channel in which a transmitter (Alice) is equipped with multiple antennas trying to communicate with a legitimate receiver (Bob) confidentially, while a passive eavesdropper (Eve) exists who is trying to wiretap the confidential information between Alice and Bob. Actually, by complementing existing cryptography-based secrecy techniques, PLS has improved the overall secure performance of a wide range of applications of RF wireless communication [10]. However, for particular constraints on the emitted signals in VLC systems, such as the average optical power, peak optical power and electrical power, instead of directly transplanting those PLS techniques developed for RF wireless communication systems, specific designs should

be proposed to the VLC scenarios to avoid opening new vulnerabilities.

Up to now, for particular interest in certain applications and convenient mathematical operation, single-input single-output (SISO) and multiple-input single-output (MISO) Gaussian wiretap channels were considered in most of the PLS aided VLC related works. Specifically, the upper and lower capacity bounds of the modulation and direct detection (IM/DD) assisted SISO VLC channel was investigated in [13]–[15]. As an extension, for the multiple-input multiple-output (MIMO) channel, authors in [16] developed the upper and lower capacity bounds with the assumption of perfect channel state information (CSI) known at the transmitter. Being one of the key techniques for achieving secrecy, multi-LEDs wiretap channel obtained particular investigation for transmission [4], [17]–[20], where the high dimensionality freedom degree could be utilized by some typical secrecy achieving strategies such as beamforming schemes [4], [19], [20] and artificial noise injection [17], [18], [21]. A scheme that jointly utilizing artificial noise and beamforming was investigated for a MISO VLC system with multiple eavesdroppers to further enhance communication secrecy [22]. Additionally, Zou et.al. in [9] have analyzed the secrecy rate of MISO optical wireless scattering communication systems, under certain constraints. Explicitly, a pair of secure communication protocols, termed as a non-jamming protocol and a cooperative jamming protocol, were proposed and tractable solutions were obtained based on the alternating optimization approach. A novel secure MIMO-VLC system has been designed using the modified Rivest-Shamir-Adleman (RSA) technique of [23] to encrypt the transmitted data in the MAC layer based on the location of the user supported by MIMO-VLC systems [23]. In [24], the closed-form analytical expressions of both secrecy outage probability and of the average secrecy capacity of a downlink VLC system have been derived by ignoring any amplitude constraints and by assuming Gaussian input distribution, while considering random positions for both the one and only legitimate user as well as for the multiple illegitimate users. By contrast, the analytical expressions of the exact and asymptotic secrecy outage probability have been derived in [25]. Light energy harvesting and random positions were assumed for the one and only legitimate user and for an illegitimate user in the context of a hybrid VLC-RF system. Additionally, the secrecy performance of MISO generalized space-shift keying (GSSK) aided VLC systems has been analyzed in [26] under certain constraints. The authors showed that without extra secrecy enhancement strategy, illegal user can easily intercept the confidential signals at high SNR region, even if its channel condition is worse than the legal user. However, there is no particular practical strategy presented for enhancing the secrecy performance except for a suggested look-up table to select the optimal LEDs in [26].

One commonality of these contributions is that the distributions of the channel input information signals and jamming signals are continuous. However, Gaussian input signal is very difficult to utilize for its infinite peak power and excessive detection complexity in VLC system. Another commonality of the above-mentioned contributions about jamming signal is that the power allocation issue between confidential signal and jamming signal is not considered, even if it is critical.

For the utilization of multiple LEDs and IM/DD techniques in the application VLC system, spatial modulation (SM) technique is inherently suited. As a result, SM aided VLC systems have been extensively studied in [27]–[29]. For SM-VLC system with discrete channel input, to the best of our knowledge, there is no achievable secrecy rate performance results about the optical jamming aided secrecy enhancement scheme and the power allocation consideration between confidential signals and optical jamming is absent yet.

B. Our Work and Contribution

Motivated by the aforementioned issues about PLS techniques, in this paper, we consider the PLS issue in SM-VLC system for secrecy performance enhancement with optical jamming. Our objective is to analysis the secrecy performance of the SM-VLC system with friendly optical jamming and propose a secrecy enhancement strategy for the proposed SM-VLC system. The contributions of this paper can be summarized as follows.

- A SM-VLC system with Gaussian wiretap channel is firstly established. A friendly optical jamming aided secrecy enhancement scheme is designed for the proposed SM-VLC system, in which Alice transmits optical jamming superimposed on the confidential signal through its LEDs. By the proposed strategy, Alice transmits the modulated signal jointly with optical jamming generated in the null space of the Alice-to-Bob channel. On one hand, with the CSI knowledge of Alice-to-Bob link, the proposed secrecy enhancement scheme does not make any change to the signals received by Bob. On the other hand, the eavesdropper will suffer from this intentional presence of optical jamming regardless of its position, as Bob does not share the exact CSI with Eve. Wherein, we adopt the truncated Gaussian distribution for optical jamming to satisfy the amplitude constraint.
- The secrecy performance of the SM-VLC system with optical jamming is analyzed, which includes the average mutual information (AMI), lower bound on AMI and its closed-form expression approximation and achievable secrecy rate. In addition, closed-form approximations for the AMI of Alice-to-Bob and Alice-to-Eve are derived, respectively. Furthermore, the influence of the peak optical intensity constraint of the

optical jamming is discussed, which involves the derivation of the probability density function (PDF) of the sum of **independent truncated Gaussian distributed variables with different variances**, where an approximation is proposed to obtain a closed-form expression.

- The power allocation strategy for the proposed optical jamming based SM-VLC system is considered, which is addressed between confidential information and interference transmission for maximizing the achievable secrecy rate of the system under amplitude and power constraints. Specially, the trade-off between the secrecy performance and the bit error rate (BER) performance is carefully considered by extended simulations. Based on our analysis, a look-up table can be constructed to guide the optimal system parameters design of the optical jamming aided SM-VLC system considered.

C. Organization and Notation

The remainder of this paper is organized as follows. The system and channel models are described in Section II. In Section III, the secrecy enhancement strategy for SM-VLC system is proposed by utilizing the optical jamming strategy, where the corresponding secrecy performance is analyzed. Then, in Section IV, the power allocation strategy between confidential information and interference transmission is considered. The simulation performance results and discussions are provided in Section V. Finally, we show our concluding remarks in Section VI.

Notation: Vectors (matrices) are denoted by boldface lowercase (uppercase) letters. The set of N-dimensional real-valued (non-negative) numbers is denoted by $\mathbb{R}^N(\mathbb{R}_+^N)$. $|\cdot|$, $\|\cdot\|$, $(\cdot)^{\mathrm{T}}$, $\lfloor\cdot\rfloor$, $\odot$, $\mathbb{E}\{\cdot\}$, $\mathbb{I}(\cdot;\cdot)$, $\binom{\cdot}{\cdot}$ denote absolute value, Euclidean norm, transposition, floor operation, Hadamard product, expected value, mutual information, and binomial coefficient, respectively. We use $\mathbf{I}_N$ and $\mathbb{1}$ to denote the N-dimensional identity matrix and the all-one column vector of length N, respectively. The curled inequality symbol $\preceq$ between two vectors denotes componentwise inequality. Superscript $[x]^+$ denotes $\max\{x, 0\}$. A lowercase letter x, y, z denotes one realization of the random variable X, Y, Z, respectively. **The transmitter is denoted as Alice. Legitimate user and illegitimate user are denoted as Bob and Eve, respectively.** We use the subscripts $(\cdot)_{\mathrm{B}}$ and $(\cdot)_{\mathrm{E}}$ to denote relevance to Bob and Eve, respectively.

II. VLC System Description and Channel Models

In this paper, a VLC system utilizing IM/DD is considered, we assume that the confidential information is transmitted from a transmitter Alice to a legitimate receiver Bob under an

eavesdropper Eve. We further assume that the transmitter is equipped with N_t down-facing LEDs installed on the ceiling, which are used to communicate privately with Bob, who has only one photo-detector (PD) fixed in up-facing. There is an eavesdropper Eve, which is also equipped with a single PD, who attempts to intercept the confidential information sent from Alice to Bob. For simplicity, the PD of Eve is also assumed to face upwards, although this is not necessary. Furthermore, all the LEDs and PDs are assumed to have the same parameters in this paper.

Therefore, the VLC system considered represents a typical multiple-input single-output single-Eve (MISOSE) VLC Gaussian wiretap channel model. The observed signals by Bob and Eve are expressed, respectively, as

$$y = \mathbf{h}_{\mathrm{B}}^{\mathrm{T}}\mathbf{x} + w_{\mathrm{B}}, \tag{1}$$

$$z = \mathbf{h}_{\mathrm{E}}^{\mathrm{T}}\mathbf{x} + w_{\mathrm{E}}, \tag{2}$$

where, by definition, $\mathbf{h}_{\mathrm{B}} = [h_{\mathrm{B},1}, h_{\mathrm{B},2}, \cdots, h_{\mathrm{B},N_t}]^{\mathrm{T}} \in \mathbb{R}_+^{N_t}$ and $\mathbf{h}_{\mathrm{E}} = [h_{\mathrm{E},1}, h_{\mathrm{E},2}, \cdots, h_{\mathrm{E},N_t}]^{\mathrm{T}} \in \mathbb{R}_+^{N_t}$, which represent the channel gains of the Alice-to-Bob link and Alice-to-Eve link, respectively. We assume that Alice has the full knowledge of $\mathbf{h}_{\mathrm{B}}$ but no knowledge about $\mathbf{h}_{\mathrm{E}}$. Eve is able to estimate its own channel vector $\mathbf{h}_{\mathrm{E}}$. The information-bearing signal vector sent by Alice $\mathbf{x} = [x_1, x_2, \cdots, x_{N_t}]^{\mathrm{T}} \in \mathbb{R}^{N_t}$, as in (1) and (2), is assumed to be a signal vector superimposed on an identical direct current (DC) bias $I_{\mathrm{DC}} \in \mathbb{R}_+$ for the purpose to adjust the illumination level of LEDs [4]. For the sake of safety, avoiding clipping distortion and preserving battery, the total current $I_{\mathrm{DC}} + x_i$ is restricted within the range of $[(1-\alpha)I_{\mathrm{DC}}, (1+\alpha)I_{\mathrm{DC}}]$, where $\alpha \in [0, 1]$ is referred to as the modulation index [13], [4]. As a result, the information-bearing signal x_i has to satisfy the peak amplitude constraint of $|x_i| \leq A, \forall i$ with $A = \alpha I_{\mathrm{DC}} \in \mathbb{R}_+$. Finally, in (1) and (2), $w_{\mathrm{B}} \sim \mathcal{N}(0, \sigma_{\mathrm{B}}^2)$ and $w_{\mathrm{E}} \sim \mathcal{N}(0, \sigma_{\mathrm{E}}^2)$ are zero-mean additive white Gaussian noise (AWGN), received at Bob and Eve, respectively.

In indoor VLC, with a generalized Lambertian emission pattern, the path gain $G_{\mathrm{B},i}$ between the i-th LED and the PD of Bob can be expressed as [4], [30],

$$G_{\mathrm{B},i} = \begin{cases} \frac{1}{2\pi d_i^2}(L+1)A_{\mathrm{Rx}}\cos^L(\phi)\cos\psi_i, & \text{if } \ 0 \leq |\psi_i| \leq \Psi_{\mathrm{FoV}}, \\ 0, & \text{if } \ |\psi_i| > \Psi_{\mathrm{FoV}}, \end{cases} \tag{3}$$

where $L = -1/\log_2\left(\cos\Phi_{1/2}\right)$ is the order of Lambertian emission with half irradiance at semi-angle $\Phi_{1/2}$, which is measured from the optical axis of the LED, d_i is the LoS distance between the i-th LED and the PD, ϕ is the angle of irradiance of LED, ψ_i is the angle of incidence of the i-th optical link, which is measured from the axis normal to the receiver surface,and Ψ_{FoV} is the receiver's field-of-view (FoV) semi-angle. Finally, $A_{\mathrm{R}x}$ is the effective

detection area of PD, which is given by [30]

$$A_{\mathrm{Rx}} = \frac{\beta^2}{\sin^2(\Psi_{\mathrm{FoV}})} A_{\mathrm{PD}}, \tag{4}$$

where β is the refractive index of the optical concentrator and A_{PD} is the PD area. As a whole, the VLC channel gain between the i-th LED and the PD of Bob can be expressed as

$$h_{\mathrm{B},i} = TRG_{\mathrm{B},i}\eta, \quad i = 1, 2, \cdots, N_t, \tag{5}$$

where T is the gain of a transimpedance amplifier, R is the responsivity of the PD and η is the current-to-light conversion efficiency of the LEDs, respectively. Similarly, the channel gain between the i-th LED and the PD of Eve can be expressed as $h_{\mathrm{E},i} = TRG_{\mathrm{E},i}\eta$, for $i = 1, 2, \cdots, N_t$.

Note that, from Eq. (3), we can readily conclude that the VLC channel gain $h_{\mathrm{B},i}$ or $h_{\mathrm{E},i}$ depend on the specific position of the transmitter LED and the receiver PD. **If an LED is not in a receiver's FoV**, the channel gain of the link will be zero [4]. Additionally, if light reflections from interior surfaces of the service area are considered, to obtain an accurate VLC channel, both the LoS link and the non-LoS links should be investigated. However, the power conveyed by the non-LoS links is in general significantly smaller than that conveyed by the LoS one [4], [31]. Consequently, when considering that the transmit LEDs are installed on the ceiling of the service area and face down-forwards, the channel model in Eq. (3) can neglect the non-LoS components, but consider only the LoS component for carrying out tractable analysis. We note furthermore that the focus of this paper is on PLS, and we hence ignore the room-specific reflections for the sake of simplicity of analysis.

III. Performance Analysis of the Optical Jamming Aided SM-VLC System

In this section, by exploiting the optical jamming approach, the secrecy performance of the proposed SM-VLC system is considered. The signal model and SM-VLC system are introduced, firstly. Then, the optical jamming aided SM-VLC scheme is designed for secrecy performance enhancement. After that, the secrecy performance of the optical jamming aided SM-VLC system is analyzed systematically. Finally, the error performance of the proposed SM-VLC system is provided.

A. SM-VLC System and Signals Modelling

Let us assume that there are N LEDs in the considered service area. For our proposed SM-VLC system, we assume that $N_t (N_t \leq N)$ LEDs are utilized for implementation of the SM modulation among the N LEDs. During one specific symbol duration, among the selected

N_t transmit LEDs, one LED are activated to transmit a specific information symbol, while the rest $(N_t - 1)$ LEDs are only used for illumination. Hence, there are in total N_t possible cases. In the following part of this paper, we assume that N_t is the power of 2 without loss of generality, therefore, $N_t = 2^{m_l}$ with $m_l \in \mathbb{R}_+$ are used for information modulation configuration. Furthermore, the length of the remaining bits per symbol is $m_s = \log_2(M)$, where M is the order of the IM pulse amplitude modulation (PAM) constellation and is also assumed to be the power of 2, and we further assume that $\mathcal{S} = \{s_m\}_{m=1}^{M}$, where $s_m = \frac{2Im}{M+1}$ for $m = 1, 2, \cdots, M$, I is the mean optical intensity emitted [32]. Therefore, the number of binary bits per SM symbol is $n_{\text{SM}} = m_l + m_s = \log_2(N_t) + \log_2(M) = \log_2(N_t M)$.

Specifically, we assume that an independent and identically distributed (i.i.d.) random bit sequence $\{\cdots, b_1, b_2, \cdots, b_r, \cdots\}$ puts into the SM mapper, where the bit sequence is divided into blocks of $n = \log_2(N_t M)$ bits that are mapped into the SM symbols $\mathbf{x}, \mathbf{x} \in \mathcal{X}$, and $\mathcal{X}$ is the $N_t M$ SM symbols set. Aided by $\mathbf{x}$, special LED is selected to transmit a symbol with particular optical intensity chosen from the set of $\mathcal{S}$. An example of portraying an SM-VLC system is demonstrated in Fig. 1, where $N_t = 4, m_l = 2, M = 4, m_s = 2, n_{\text{SM}} = 4$. The bit sequence to be transmitted is grouped into a fixed length of 4 bits, which is determined by the number of selected transmit LEDs N_t and signal constellation size M. During a symbol period, we assume that the incoming bit sequence to the encoder is $\{\cdots, 0000, 0110, 1101, 1011, \cdots\}$, then the bits at each time instant are mapped to a special transmitting LED and a special signal constellation point. Consequently, the selected LED will transmit the signal with a special intensity $s_m, m = 1, 2, \cdots, M$ at this particular time instant and all other LEDs remain silent.

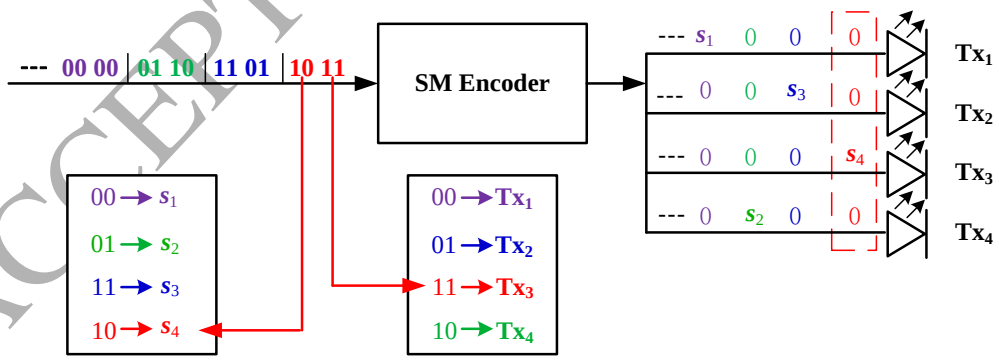

Fig. 1. Demonstration of SM-VLC modulation providing 4bit/s/Hz with $N_t = 4, M = 4$.

Hence, the transmitted SM-VLC signal vector $\mathbf{x}$ can be expressed as

$$\mathbf{x} = \mathbf{e}_{n_t} s_m = [0 \ \cdots \ 0 \ \underbrace{s_m}_{n_t\text{-th}} \ 0 \ \cdots \ 0]^{\mathrm{T}}, \tag{6}$$

where $\mathbf{e}_{n_t}$, $n_t \in \{1, 2, \cdots, N_t\}$, represents one specific column of an identity matrix $\mathbf{I}_{N_t} = [\mathbf{e}_1, \mathbf{e}_2, \cdots, \mathbf{e}_{N_t}]$, which column is determined by the index of the n_t-th activated LED. Without loss of generality, we assume that the average power constraint of $\mathbf{x}$ is $\mathbb{E}\{\|\mathbf{x}\|^2\} = \mathcal{P}$, as well as that we have $|\mathbf{x}| \preceq A\mathbf{1}$ for our peak amplitude constraint, where $\mathcal{P}$ is the total power per transmission and $A = \alpha I_{\text{DC}}$.

Note that, the above-described SM-VLC system is reduced to the space shift keying (SSK) VLC system, when $M = 1$. Therefore, the SSK-VLC scheme is a special case of our SM-VLC, and hence, all the following analysis and results can be straightforwardly applied to the SSK-VLC by letting $M = 1$.

When the signal of (6) is transmitted over the VLC wiretap channel, following (1) and (2), we have

$$y = \mathbf{h}_{\text{B}}^{\text{T}}\mathbf{x} + w_{\text{B}} = \mathbf{h}_{\text{B}}^{\text{T}}\mathbf{e}_{n_t}s_m = h_{\text{B},n_t}s_m + w_{\text{B}}, \tag{7}$$

$$z = \mathbf{h}_{\text{E}}^{\text{T}}\mathbf{x} + w_{\text{E}} = \mathbf{h}_{\text{E}}^{\text{T}}\mathbf{e}_{n_t}s_m = h_{\text{E},n_t}s_m + w_{\text{E}}, \tag{8}$$

where by definition, $h_{\text{B},n_t} = \mathbf{h}_{\text{B}}^{\text{T}}\mathbf{e}_{n_t}$ and $h_{\text{E},n_t} = \mathbf{h}_{\text{E}}^{\text{T}}\mathbf{e}_{n_t}$.

B. SM-VLC System with Optical Jamming

In this subsection, we commence to enhance the secrecy performance of the Alice-to-Bob link, by exploiting the optical jamming on Eve's reception and hence degrading its signal-to-interference-plus-noise ratio (SINR). In a practical SM-VLC system, it is reasonable to assume that Alice does not have the CSI about the Alice-to-Eve link for a passive eavesdropper. However, Alice may transmit an optical jamming along with the information modulated SM signal in the nullspace of the Alice-to-Bob channel. In principle, at any time instance, besides Alice transmits a symbol using a special selected LED, all the other $N_t - 1$ LEDs can simultaneously be utilized to tranmsmit optical jamming without interfering the reception at Bob. In this case, Bob is capable of receiving its confidential information as in the conventional SM system, while Eve experiences the intentional interference sent by Alice. Hence the secrecy performance can be enhanced without adding any burden on Bob's reception. However, the enhancement of secrecy performance is at the cost of activating more LEDs, and of assigning additional power for emitting jamming under the constraint of the same total power.

The system model of the SM-VLC system with optical jamming is depicted in Fig. 2. With the aid of the singular value decomposition (SVD) [33], the VLC channel gain of the Alice-to-Bob link can be expressed $\mathbf{h}_{\text{B}}$ as

$$\mathbf{h}_{\text{B}}^{\text{T}} = [\lambda, \mathbf{0}^{\text{T}}][\mathbf{v}_s, \mathbf{V}_n]^{\text{T}}, \tag{9}$$

where λ is the singular value, $\mathbf{v}_s$ **is the right singular vector associated to singular value** λ **of the VLC channel gain** $\mathbf{h}_\mathrm{B}$. From (9), we obtain a null space $\mathbf{V}_n = [\mathbf{v}_1, \mathbf{v}_2, \cdots, \mathbf{v}_{N_t-1}] \in \mathbb{R}^{N_t \times (N_t-1)}$ as $\mathbf{h}_\mathrm{B}$ has $\mathrm{rank}(\mathbf{h}_\mathrm{B}) = 1$. Then, the optical jamming emitted by Alice can be designed as

$$\mathbf{w} = \mathbf{V}_n \mathbf{u}, \tag{10}$$

where $\mathbf{u} = [u_1, u_2, \cdots, u_{N_t-1}]^\mathrm{T} \in \mathbb{R}^{N_t-1}$ is a time-varying jamming vector, whose entries are assumed to comply with a real truncated Gaussian distribution [34] over the interval of $[-\frac{A_2}{N_t-1}, \frac{A_2}{N_t-1}]$. Thus, the peak amplitude constraint of the (N_t-1) jamming codewords in every transmission is in the interval $[-A_2, +A_2]$. Then, we denote the peak amplitude constraint of the confidential signal as A_1 Thus, the whole peak amplitude constraint of the output intensity of the LEDs can be expressed as $A = A_1 + A_2$.

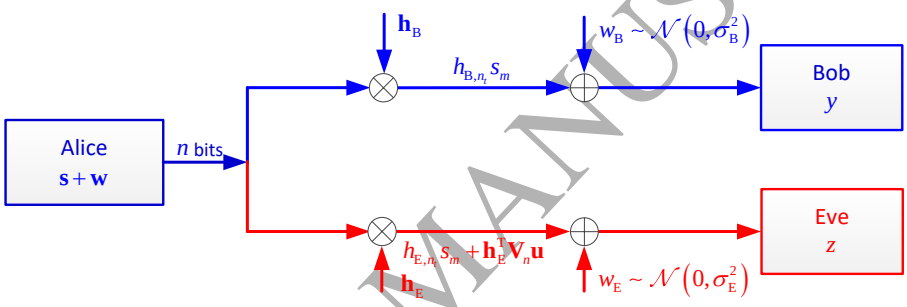

Fig. 2. System model of the SM-VLC Gaussian wiretap channel with optical jamming.

We assume that $\tilde{P}$ is a Gaussian distributed real random variable defined as $\tilde{P} \sim \mathcal{N}(\mu, \sigma^2)$, then the double-sided truncated Gaussian random variable of $\tilde{P}$ is denoted as P, whose PDF is expressed as $\mathcal{TN}(\mu, \sigma^2, -B, B)$, and is given by

$$f_P(p) = \frac{\frac{1}{\sqrt{2\pi\sigma^2}} \exp\left(\frac{-(p-\mu)^2}{2\sigma^2}\right)}{\Phi\left(\frac{B-\mu}{\sigma}\right) - \Phi\left(\frac{-B-\mu}{\sigma}\right)} I_{[-B,B]}(p), \tag{11}$$

where $\Phi(\cdot)$ is the Gaussian cumulative distribution function (CDF), $I_{[-B,B]}(p)$ is the indicator function satisfying $I_{[-B,B]}(p) = 1$ if $p \in [-B, B]$ and $I_{[-B,B]}(p) = 0$, otherwise. Following this, in our scheme, we set $u_i \sim \mathcal{TN}(0, \frac{\sigma_J^2}{N_t-1}, -\frac{A_2}{N_t-1}, \frac{A_2}{N_t-1}), i = 1, 2, \cdots, N_t - 1$.

By adding the optical jamming, the transmitting signals from the N_t LEDs of Alice can be expressed as

$$\mathbf{x} = \mathbf{s} + \mathbf{w} = s_m \mathbf{e}_{n_t} + \mathbf{V}_n \mathbf{u}. \tag{12}$$

We assume that $\mathbb{E}\{\mathbf{s}^{\mathrm{T}}\mathbf{s}\} = s^2$, then in the SM-VLC system considered, the total transmit power is constrained by

$$\mathbb{E}\{\|\mathbf{x}\|^2\} = \mathbb{E}\{\mathbf{x}^{\mathrm{T}}\mathbf{x}\} = \mathbb{E}\{\mathbf{s}^{\mathrm{T}}\mathbf{s} + \mathbf{w}^{\mathrm{T}}\mathbf{w}\} = s^2 + \sigma_J^2 = \mathcal{P}. \tag{13}$$

Hence, the optical power can be assigned to transmit confidential signals and optical jamming by adjusting s^2 and σ_J^2 in (13). Consequently, the observations attained by Bob and Eve can be expressed as, respectively

$$y = \mathbf{h}_{\mathrm{B}}^{\mathrm{T}}\mathbf{x} + w_{\mathrm{B}} = \mathbf{h}_{\mathrm{B}}^{\mathrm{T}}\mathbf{e}_{n_t}s_m + \mathbf{h}_{\mathrm{B}}^{\mathrm{T}}\mathbf{w} + w_{\mathrm{B}} = h_{\mathrm{B},n_t}s_m + w_{\mathrm{B}}, \tag{14}$$

$$z = \mathbf{h}_{\mathrm{E}}^{\mathrm{T}}\mathbf{x} + w_{\mathrm{E}} = \mathbf{h}_{\mathrm{E}}^{\mathrm{T}}\mathbf{e}_{n_t}s_m + \mathbf{h}_{\mathrm{E}}^{\mathrm{T}}\mathbf{w} + w_{\mathrm{E}} = h_{\mathrm{E},n_t}s_m + \mathbf{h}_{\mathrm{E}}^{\mathrm{T}}\mathbf{V}_n\mathbf{u} + w_{\mathrm{E}}, \tag{15}$$

where we have (14) owing to $\mathbf{h}_{\mathrm{B}}$ is orthogonal to $\mathbf{w}$. From (14) and (15) indicate, the secrecy performance of Bob and Eve in the considered SM-VLC system is the same, if there is no added optical jamming on Eve's reception. However, when there is optical jamming provided by $\mathbf{w}$, Bob's reception is not affected, apart from the allocation of a portion of the power to optical jamming, while Eve's reception may be severely discharged, resulting in an improved secrecy performance for Bob, which will be experimentally verified in the simulations.

C. Secrecy Performance Analysis of Optical Jamming Aided SM-VLC System

In the following of this subsection, we derive the AMI between Alice and Eve of the SM-VLC system considered. Based on the aforementioned results, we can then obtain the AMI between Alice and Bob by letting $\mathbf{w} = \mathbf{0}$. Firstly, we give the scheme of generating optical jamming signals. Let $\breve{w}_{\mathrm{E}}$ denote the equivalent noise observed by Eve. Then, from (15), we have

$$\breve{w}_{\mathrm{E}} = \mathbf{h}_{\mathrm{E}}^{\mathrm{T}}\mathbf{w} + w_{\mathrm{E}} = \mathbf{h}_{\mathrm{E}}^{\mathrm{T}}\mathbf{V}_n\mathbf{u} + w_{\mathrm{E}} = \sum_{i=1}^{N_t-1} u_i\mathbf{h}_{\mathrm{E}}^{\mathrm{T}}\mathbf{v}_i + w_{\mathrm{E}}, \tag{16}$$

which is the sum of $N_t - 1$ independent distributed variables with different variances. Since for the convolution of a set of double-sided truncated Gaussian variables, the distribution of $\breve{w}_{\mathrm{E}}$ is very difficult to derive a closed-form of PDF expression. For example, even for the sum of two variables obeying the double-sided truncated Gaussian distribution, the PDF resultant is very complicated. Specifically, let $X_1 \sim \mathcal{TN}(\mu_{x_1}, \sigma_{x_1}, a_{x_1}, b_{x_1}), X_2 \sim \mathcal{TN}(\mu_{x_2}, \sigma_{x_2}, a_{x_2}, b_{x_2})$ and $f_i(x_i, \mu_i, \sigma_i) = \frac{1}{\sqrt{2\pi}\sigma_i}e^{-\frac{(x_i-\mu_i)^2}{2\sigma_i^2}}$, as well as denote $Z_1 = X_1 + X_2$. Then, the PDF of Z_1 is in the form of

$$f_{Z_1}(z_1) = \frac{\int_{\delta_1}^{\delta_2} f_1 f_2 dx_1}{\Phi_1\Phi_2}, \tag{17}$$

where $\delta_1 = \max\{a_{x_1}, z_1 - b_{x_2}\}, \delta_2 = \min\{b_{x_1}, z_1 - a_{x_2}\}, f_1 = f(x_1, \mu_{x_1}, \sigma_{x_1}), f_2 = f(z_1 - x_1, \mu_{x_2}, \sigma_{x_2}), \Phi_1 = \Phi(b_{x_1}, \mu_{x_1}, \sigma_{x_1}) - \Phi(a_{x_1}, \mu_{x_1}, \sigma_{x_1}), \Phi_2 = \Phi(b_{x_2}, \mu_{x_2}, \sigma_{x_2}) - \Phi(a_{x_2}, \mu_{x_2}, \sigma_{x_2})$. Furthermore, for deriving the PDF of $\breve{w}_{\mathrm{E}}$, we need to compute the convolution of $f_{Z_1}(z_1)$ and the PDF of a Gaussian distributed w_{E}, which is too complicated to simplify. **Because of the above-mentioned, we apply the Lyapunov central limit theorem, which states that the sum of T independent distributed variables follows an approximate Gaussian distribution as T becomes large**. In practice, the number of transmit LEDs is usually large, and therefore we can be confident that $\breve{w}_{\mathrm{E}}$ has a near-Gaussian distribution.

When we invoke the **Lyapunov** central limit theorem in our analysis, we have the following simulations and hypothesis tests to support our analysis. **For example, we assume that** 10 **independent truncated Gaussian distributed random variables obeying the distribution** $Z_i \sim \mathcal{TN}(\mu_i, \sigma_i, a_i, b_i)$ **are considered, where we have** $\mu_i = 0, \sigma_i \sim \mathcal{N}(1, 10^{-4}), a_i = -5, b_i = 5, i = 1, \cdots, 10$**. Note that, the variance of** Z_i **is approximated by the fact that the Eve's channel gain of the considered VLC system is usually less than** 10^{-4} **[4]. The histogram of the sum of these random variables** $Z = \frac{\sum_{i=1}^{10}(Z_i - \mu_i)}{\sqrt{\sum_{i=1}^{10}\sigma_i^2}}$ **is shown in Fig. 3.** Clearly, it is quite close to the Gaussian distribution.

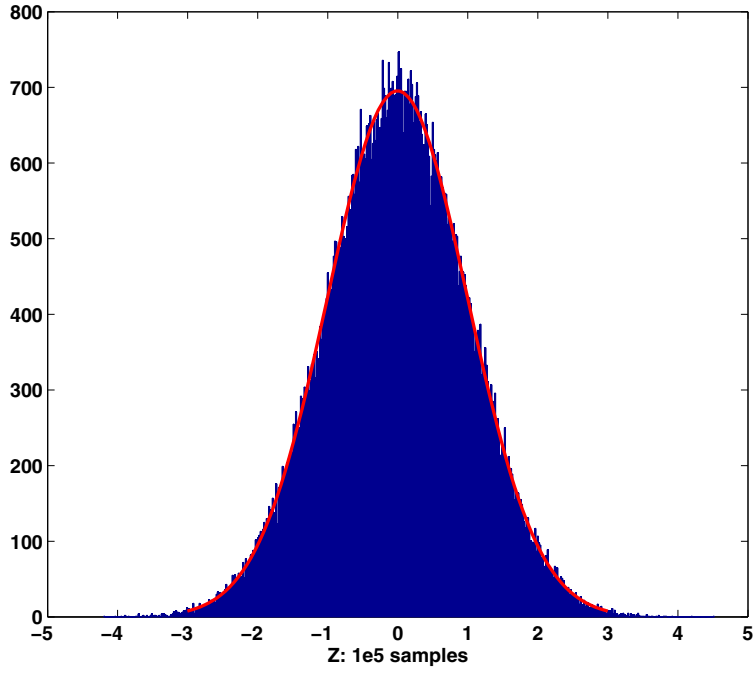

Fig. 3. **The `histfit` plot of the sum of** 10 **independent truncated Gaussian distributed random variables with different variances. The approximated mean and standard deviation of** Z **are** $\mu_Z = 0.0027$ **and** $\sigma_Z = 0.9970$**.**

Then, a hypothesis test approach, termed as the Jarque-Bera test [35], is executed to test the hypothesis that the distribution of the sum of 10 independent truncated Gaussian random

variables is a Gaussian distribution at the 5% significance level. Given the above-mentioned parameters and assuming that the number of processes is higher than or equal to 10, the test always returns the null hypothesis. For practical applications, in order to obtain adequate illumination of a certain room, there are always multiple LEDs. It is very common to use more than 10 LEDs. As a result, from the above mentioned analysis, invoking the **Lyapunov** central limit theorem to approximate the sum of independent truncated Gaussian random variables with different variances as a Gaussian distribution variable is reasonable for our SM-VLC systems.

With the aid of the Gaussian approximation, it is easy argue that the mean of $\breve{w}_{\mathrm{E}}$ is zero, while has a covariance of

$$\begin{aligned}\Omega_{\mathrm{E}} &\overset{(a)}{=} \mathbb{E}\left\{\left(\mathbf{h}_{\mathrm{E}}^{\mathrm{T}}\sum_{i=1}^{N_t-1}u_i\mathbf{v}_i\right)\left(\mathbf{h}_{\mathrm{E}}^{\mathrm{T}}\sum_{j=1}^{N_t-1}u_j\mathbf{v}_j\right)^{\mathrm{T}}\right\}+\sigma_{\mathrm{E}}^2 \\ &= \frac{\sigma_J^2}{N_t-1}\mathbf{h}_{\mathrm{E}}^{\mathrm{T}}\left(\sum_{i=1}^{N_t-1}\mathbf{v}_i\mathbf{v}_i^{\mathrm{T}}\right)\mathbf{h}_{\mathrm{E}}+\sigma_{\mathrm{E}}^2 = \frac{\sigma_J^2}{N_t-1}\mathbf{h}_{\mathrm{E}}^{\mathrm{T}}\mathbf{V}_n\mathbf{V}_n^{\mathrm{T}}\mathbf{h}_{\mathrm{E}}+\sigma_{\mathrm{E}}^2. \end{aligned} \tag{18}$$

where we have the equality (a) is because $\{u_i\}_{i=1}^{N_t-1}$ and w_{E} are statistically independent. Consequently, the received signal of Eve can be expressed as

$$z = h_{\mathrm{E},n_t}s_m + \breve{w}_{\mathrm{E}}. \tag{19}$$

Then, by manipulating a normalizing factor $\Omega_{\mathrm{E}}^{-1/2}$, the equivalent noise $\breve{w}_{\mathrm{E}}$ is whitened. As a result, the whitened equivalent noise can be describes as $\tilde{w}_{\mathrm{E}}(t) = \Omega_{\mathrm{E}}^{-1/2}\breve{w}_{\mathrm{E}}(t)$. Finally, after normalizing z by multiplying $\Omega_{\mathrm{E}}^{-1/2}$, we have

$$\tilde{z} = \Omega_{\mathrm{E}}^{-1/2}h_{\mathrm{E},n_t}s_m + \Omega_{\mathrm{E}}^{-1/2}\breve{w}_{\mathrm{E}} = \tilde{h}_{\mathrm{E},n_t}s_m + \tilde{w}_{\mathrm{E}}, \tag{20}$$

where $\tilde{w}_{\mathrm{E}}$ is zero mean and unit variance, and by definition, $\tilde{h}_{\mathrm{E},n_t} = \Omega_{\mathrm{E}}^{-1/2}h_{\mathrm{E},n_t}$. Consequently, the conditional and unconditional PDFs of Eve's received signal $\tilde{z}$ can be expressed as

$$p_{\tilde{Z}|\tilde{\mathbf{h}}_{\mathrm{E}},S}(\tilde{z}|\tilde{h}_{\mathrm{E}} = \tilde{h}_{\mathrm{E},n_t}, s = s_m) = \frac{1}{\sqrt{2\pi}}\exp\left(-\frac{1}{2}(\tilde{z}-\tilde{h}_{\mathrm{E},n_t}s_m)^2\right). \tag{21}$$

$$p_{\tilde{Z}|S}(\tilde{z}|s = s_m) = \frac{1}{N_t}\sum_{n_t=1}^{N_t}\frac{1}{\sqrt{2\pi}}\exp\left(-\frac{1}{2}(\tilde{z}-\tilde{h}_{\mathrm{E},n_t}s_m)^2\right). \tag{22}$$

$$p_{\tilde{Z}|\tilde{\mathbf{h}}_{\mathrm{E}}}(\tilde{z}|\tilde{h}_{\mathrm{E}} = \tilde{h}_{\mathrm{E},n_t}) = \frac{1}{M}\sum_{m=1}^{M}\frac{1}{\sqrt{2\pi}}\exp\left(-\frac{1}{2}(\tilde{z}-\tilde{h}_{\mathrm{E},n_t}s_m)^2\right). \tag{23}$$

$$p_{\tilde{Z},\tilde{\mathbf{h}}_{\mathrm{E}}|S}(\tilde{z},\tilde{h}_{\mathrm{E},n_t}|s=s_m)=p_{\tilde{Z}|\tilde{\mathbf{h}}_{\mathrm{E}},S}(\tilde{z}|\tilde{h}_{\mathrm{E}}=\tilde{h}_{\mathrm{E},n_t},s=s_m)P_{\tilde{\mathbf{h}}_{\mathrm{E}}|S}(\tilde{h}_{\mathrm{E},n_t}|s=s_m)$$
$$=\frac{1}{N_t}\frac{1}{\sqrt{2\pi}}\exp\left(-\frac{1}{2}(\tilde{z}-\tilde{h}_{\mathrm{E},n_t}s_m)^2\right). \tag{24}$$

$$p_{\tilde{Z}}(\tilde{z})=\frac{1}{MN_t}\sum_{m=1}^{M}\sum_{n_t=1}^{N_t}\frac{1}{\sqrt{2\pi}}\exp\left(-\frac{1}{2}(\tilde{z}-\tilde{h}_{\mathrm{E},n_t}s_m)^2\right). \tag{25}$$

respectively. Similarly, the conditional and unconditional PDFs of y can be respectively expressed as

$$p_{Y|\mathbf{h}_{\mathrm{B}},S}(y|h_{\mathrm{B}}=h_{\mathrm{B},n_t},s=s_m)=\frac{1}{\sqrt{2\pi}\sigma_{\mathrm{B}}}\exp\left(-\frac{(y-h_{\mathrm{B},n_t}s_m)^2}{2\sigma_{\mathrm{B}}^2}\right). \tag{26}$$

$$p_{Y|S}(y|s=s_m)=\frac{1}{N_t}\sum_{n_t=1}^{N_t}\frac{1}{\sqrt{2\pi}\sigma_{\mathrm{B}}}\exp\left(-\frac{(y-h_{\mathrm{B},n_t}s_m)^2}{2\sigma_{\mathrm{B}}^2}\right). \tag{27}$$

$$p_{Y|\mathbf{h}_{\mathrm{B}}}(y|h_{\mathrm{B}}=h_{\mathrm{B},n_t})=\frac{1}{M}\sum_{m=1}^{M}\frac{1}{\sqrt{2\pi}\sigma_{\mathrm{B}}}\exp\left(-\frac{(y-h_{\mathrm{B},n_t}s_m)^2}{2\sigma_{\mathrm{B}}^2}\right). \tag{28}$$

$$p_{Y,\mathbf{h}_{\mathrm{B}}|S}(y,h_{\mathrm{B},n_t}|s=s_m)=p_{Y|\mathbf{h}_{\mathrm{B}},S}(y|h_{\mathrm{B}}=h_{\mathrm{B},n_t},s=s_m)P_{\mathbf{h}_{\mathrm{B}}|S}(h_{\mathrm{B},n_t}|s=s_m)$$
$$=\frac{1}{N_t}\frac{1}{\sqrt{2\pi}\sigma_{\mathrm{B}}}\exp\left(-\frac{(y-h_{\mathrm{B},n_t}s_m)^2}{2\sigma_{\mathrm{B}}^2}\right). \tag{29}$$

$$p_Y(y)=\frac{1}{MN_t}\sum_{m=1}^{M}\sum_{n_t=1}^{N_t}\frac{1}{\sqrt{2\pi}\sigma_{\mathrm{E}}}\exp\left(-\frac{(y-h_{\mathrm{B},n_t}s_m)^2}{2\sigma_{\mathrm{B}}^2}\right). \tag{30}$$

For the following analysis, we define $\varrho_{\mathrm{B}}=1/\sigma_{\mathrm{B}}^2$ and $\varrho_{\mathrm{E}}=1/\sigma_{\mathrm{E}}^2$ as the average signal-to-noise ratios (SNRs) at Bob and Eve, respectively. According to [36], the AMI between two probability spaces is invariant after a reversible transformation, meaning that transformation of (20) does not change the AMI. Consequently, with the PDF expressions of (26)-(29), the AMIs of both the Alice-to-Bob link and the Alice-to-Eve link can be obtained, which are stated in Theorem 1.

Theorem 1: For the considered SM-VLC system with optical jamming and finite discrete inputs, the AMI of Alice-to-Bob channel is

$$\mathbb{I}^J(S,\mathbf{h}_{\mathrm{B}};Y)=\log_2 MN_t$$
$$-\frac{1}{MN_t}\sum_{m_\tau=1}^{M}\sum_{n_\tau=1}^{N_t}\mathbb{E}_{w_{\mathrm{B}}}\left[\log_2\sum_{m_\kappa=1}^{M}\sum_{n_\kappa=1}^{N_t}\exp\left(-\frac{(w_{\mathrm{B}}+\zeta_{n_\tau,n_\kappa}^{m_\tau,m_\kappa})^2-w_{\mathrm{B}}^2}{2\sigma_{\mathrm{B}}^2}\right)\right], \tag{31}$$

where $\zeta_{n_\tau,n_\kappa}^{m_\tau,m_\kappa} = h_{\mathrm{B},n_\tau} s_{m_\tau} - h_{\mathrm{B},n_\kappa} s_{m_\kappa}$, and the AMI of Alice-to-Eve channel is

$$\mathbb{I}^J(S,\mathbf{h}_{\mathrm{E}};Z) = \mathbb{I}^J(S,\tilde{\mathbf{h}}_{\mathrm{E}};\tilde{Z}) = \log_2 MN_t - \frac{1}{MN_t}\sum_{m_\tau=1}^{M}\sum_{n_\tau=1}^{N_t}\mathbb{E}_{\tilde{w}_{\mathrm{E}}}\left[\log_2\sum_{m_\kappa=1}^{M}\sum_{n_\kappa=1}^{N_t}\exp\left(-\frac{1}{2}\left((\tilde{w}_{\mathrm{E}}+\Omega_{\mathrm{E}}^{-1/2}\xi_{n_\tau,n_\kappa}^{m_\tau,m_\kappa})^2-\tilde{w}_{\mathrm{E}}^2\right)\right)\right], \tag{32}$$

where $\xi_{n_\tau,n_\kappa}^{m_\tau,m_\kappa} = h_{\mathrm{E},n_\tau} s_{m_\tau} - h_{\mathrm{E},n_\kappa} s_{m_\kappa}$.

Proof: For the considered SM-VLC system, using the chain rules of mutual information [37], the AMI between the input signal of Alice and output signal of Bob can be written as

$$\mathbb{I}(S,\mathbf{h}_{\mathrm{B}};Y) = \mathbb{I}(\mathbf{h}_{\mathrm{B}};Y|S) + \mathbb{I}(S;Y), \tag{33}$$

where $\mathbb{I}(\mathbf{h}_{\mathrm{B}};Y|S)$ represents the average conditional mutual information between Y and $\mathbf{h}_{\mathrm{B}}$ given S, and $\mathbb{I}(S;Y)$ represent the AMI between S and Y. Based on (26)-(30), $\mathbb{I}(\mathbf{h}_{\mathrm{B}};Y|S)$ and $\mathbb{I}(S;Y)$ can be derived as

$$\begin{aligned}\mathbb{I}(\mathbf{h}_{\mathrm{B}};Y|S) &= \sum_{m_\tau=1}^{M}\sum_{n_\tau=1}^{N_t}\int_y p_{Y,\mathbf{h}_{\mathrm{B}}|S}(y,h_{\mathrm{B},n_\tau}|s=s_{m_\tau})\mathbf{P}_S(s_{m_\tau}) \\ &\quad\times\log_2\frac{p_{Y|\mathbf{h}_{\mathrm{B}},S}(y|h_{\mathrm{B}}=h_{\mathrm{B},n_\tau},s=s_{m_\tau})}{p_{Y|S}(y|s=s_{m_\tau})}dy \\ &= \log_2 N_t - \frac{1}{MN_t}\sum_{m_\tau=1}^{M}\sum_{n_\tau=1}^{N_t}\mathbb{E}_{W_{\mathrm{B}}}\left[\log_2\sum_{n_\kappa=1}^{N_t}\exp\left(\frac{w_{\mathrm{B}}^2-(w_{\mathrm{B}}+(h_{\mathrm{B},n_\tau}-h_{\mathrm{B},n_\kappa})s_{m_\tau})^2}{2\sigma_{\mathrm{B}}^2}\right)\right].\end{aligned} \tag{34}$$

$$\begin{aligned}\mathbb{I}(S;Y) &= \sum_{m_\tau=1}^{M}\int_y \mathbf{P}_S(s_{m_\tau})p_{Y|S}(y|s=s_{m_\tau})\log_2\frac{p_{Y|S}(y|s=s_{m_\tau})}{p_Y(y)}dy \\ &= \log_2 M - \frac{1}{MN_t} \\ &\quad\times\sum_{m_\tau=1}^{M}\sum_{n_\tau=1}^{N_t}\mathbb{E}_{W_{\mathrm{B}}}\left[\log_2\frac{\sum_{m_\kappa=1}^{M}\sum_{n_\kappa=1}^{N_t}\exp\left(-\frac{(w_{\mathrm{B}}+h_{\mathrm{B},n_\tau}s_{m_\tau}-h_{\mathrm{B},n_\kappa}s_{m_\kappa})^2}{2\sigma_{\mathrm{B}}^2}\right)}{\sum_{n_\kappa=1}^{N_t}\exp\left(-\frac{(w_{\mathrm{B}}+h_{\mathrm{B},n_\tau}s_{m_\tau}-h_{\mathrm{B},n_\kappa}s_{m_\tau})^2}{2\sigma_{\mathrm{B}}^2}\right)}\right].\end{aligned} \tag{35}$$

When Denoting $\zeta_{n_\tau,n_\kappa}^{m_\tau} = (h_{\mathrm{B},n_\tau}-h_{\mathrm{B},n_\kappa})s_{m_\tau}$, $\zeta_{n_\tau,n_\kappa}^{m_\tau,m_\kappa} = h_{\mathrm{B},n_\tau}s_{m_\tau} - h_{\mathrm{B},n_\kappa}s_{m_\kappa}$, by substituting (34) and (35) into (33), the AMI between Alice and Bob in the SM-VLC systems with finite alphabet can be expressed as

$$\mathbb{I}(S,\mathbf{h}_{\mathrm{B}};Y) = \log_2 MN_t - \frac{1}{MN_t} \times\sum_{m_\tau=1}^{M}\sum_{n_\tau=1}^{N_t}\mathbb{E}_{w_{\mathrm{B}}}\left[\log_2\sum_{m_\kappa=1}^{M}\sum_{n_\kappa=1}^{N_t}\exp\left(-\frac{(w_{\mathrm{B}}+\zeta_{n_\tau,n_\kappa}^{m_\tau,m_\kappa})^2-w_{\mathrm{B}}^2}{2\sigma_{\mathrm{B}}^2}\right)\right]. \tag{36}$$

For given $\zeta_{n_\tau,n_\kappa}^{m_\tau,m_\kappa}$, the AMI of (36) is a monotonically increasing function w.r.t. SNR ϱ_{B}. When $\varrho_{\mathrm{B}} \to \infty$ i.e. $\sigma_{\mathrm{B}}^2 = 0$, we have

$$\lim_{\varrho_{\mathrm{B}}\to\infty} \mathbb{I}(S, \mathbf{h}_{\mathrm{B}}; Y) = \log_2 MN_t, \tag{37}$$

which implies that the upper bound AMI of the Alice-to-Bob channel with finite discrete inputs is $\log_2 MN_t$.

Using the same procedure, when Denoting $\xi_{n_\tau,n_\kappa}^{m_\tau} = (h_{\mathrm{E},n_\tau} - h_{\mathrm{E},n_\kappa})s_{m_\tau}$, $\xi_{n_\tau,n_\kappa}^{m_\tau,m_\kappa} = h_{\mathrm{E},n_\tau}s_{m_\tau} - h_{\mathrm{E},n_\kappa}s_{m_\kappa}$, the AMI between Alice and Eve in the SM-VLC systems with finite discrete inputs can be expressed as

$$\mathbb{I}(S, \tilde{\mathbf{h}}_{\mathrm{E}}; \tilde{Z}) = \log_2 MN_t - \frac{1}{MN_t}\sum_{m_\tau=1}^{M}\sum_{n_\tau=1}^{N_t}\mathbb{E}_{\tilde{w}_{\mathrm{E}}}\left[\log_2 \sum_{m_\kappa=1}^{M}\sum_{n_\kappa=1}^{N_t}\exp\left(-\frac{1}{2}\left((\tilde{w}_{\mathrm{E}} + \Omega_{\mathrm{E}}^{-1/2}\xi_{n_\tau,n_\kappa}^{m_\tau,m_\kappa})^2 - \tilde{w}_{\mathrm{E}}^2\right)\right)\right]. \tag{38}$$

For given $\xi_{n_\tau,n_\kappa}^{m_\tau,m_\kappa}$, the AMI of (38) is a monotonically increasing function w.r.t. SNR Ω_{E}^{-1}. When $\Omega_{\mathrm{E}}^{-1} \to \infty$, we have $\lim_{\Omega_{\mathrm{E}}^{-1}\to\infty} \mathbb{I}(S, \tilde{\mathbf{h}}_{\mathrm{E}}; \tilde{Y}) = \log_2 MN_t$, which implies that the upper bound AMI of the Alice-to-Eve channel with finite discrete inputs is $\log_2 MN_t$.

■

Upon substituting (31) and (32) into $R_{\text{sec}}^J = [\mathbb{I}^J(h_{\mathrm{B}}; Y) - \mathbb{I}^J(h_{\mathrm{E}}; Z)]^+$, the achievable secrecy rate of the SM-VLC system can be expressed as

$$R_{sec}^J = \left[-\frac{1}{MN_t}\sum_{m_\tau=1}^{M}\sum_{n_\tau=1}^{N_t}\mathbb{E}_{w_{\mathrm{B}}}\left[\log_2 \sum_{m_\kappa=1}^{M}\sum_{n_\kappa=1}^{N_t}\exp\left(-\frac{(w_{\mathrm{B}} + \zeta_{n_\tau,n_\kappa}^{m_\tau,m_\kappa})^2 - w_{\mathrm{B}}^2}{2\sigma_{\mathrm{B}}^2}\right)\right] + \frac{1}{MN_t}\sum_{m_\tau=1}^{M}\sum_{n_\tau=1}^{N_t}\mathbb{E}_{w_{\mathrm{E}}}\left[\log_2 \sum_{m_\kappa=1}^{M}\sum_{n_\kappa=1}^{N_t}\exp\left(-\frac{(w_{\mathrm{E}} + \xi_{n_\tau,n_\kappa}^{m_\tau,m_\kappa})^2 - w_{\mathrm{E}}^2}{2\sigma_{\mathrm{E}}^2}\right)\right]\right]^+. \tag{39}$$

D. Lower-bound for AMI

Generally, deriving a closed-form expection w.r.t. w_{B} or w_{E} in (31) or (32) is not an easy task. Therefore, in stead, we below derive the lower-bounds for the AMIs of both Alice-to-Bob link and Alice-to-Eve link, which are detailed in the following theorem.

Theorem 2: The AMI between the input signal of Alice and the output signal of Bob can be lower-bounded by

$$\mathbb{I}_L(S, \mathbf{h}_{\mathrm{B}}; Y) = \log_2 MN_t - \frac{1}{2}(\log_2 e - 1) - \frac{1}{MN_t}\sum_{m_\tau=1}^{M}\sum_{n_\tau=1}^{N_t}\log_2 \sum_{m_\kappa=1}^{M}\sum_{n_\kappa=1}^{N_t}\exp\left(-\frac{(\zeta_{n_\tau,n_\kappa}^{m_\tau,m_\kappa})^2}{4\sigma_{\mathrm{B}}^2}\right). \tag{40}$$

Similarly, the AMI between the input signal of Alice and the output signal of Eve can be lower-bounded by

$$\mathbb{I}_L(S,\mathbf{h}_{\rm E};Z)=\log_2 MN_t-\frac{1}{2}(\log_2 e-1)\\ -\frac{1}{MN_t}\sum_{m_\tau=1}^{M}\sum_{n_\tau=1}^{N_t}\log_2\sum_{m_\kappa=1}^{M}\sum_{n_\kappa=1}^{N_t}\exp\left(-\frac{(\xi_{n_\tau,n_\kappa}^{m_\tau,m_\kappa})^2}{4\Omega_{\rm E}}\right). \tag{41}$$

Proof: The proof of (40) and that of (41) are similar. Therefore, in the following, we only detail the proof of (41).

From (32), we can have

$$\begin{aligned}\mathbb{I}^J(S,\mathbf{h}_{\rm E};Z)&=\log_2 MN_t-\frac{1}{MN_t}\sum_{m_\tau=1}^{M}\sum_{n_\tau=1}^{N_t}\mathbb{E}_{\tilde{w}_{\rm E}}\left[\log_2\exp\left(\frac{\tilde{w}_{\rm E}^2}{2}\right)\right]\\ &\quad-\frac{1}{MN_t}\sum_{m_\tau=1}^{M}\sum_{n_\tau=1}^{N_t}\mathbb{E}_{\tilde{w}_{\rm E}}\left[\log_2\sum_{m_\kappa=1}^{M}\sum_{n_\kappa=1}^{N_t}\exp\left(-\frac{\left(\tilde{w}_{\rm E}+\Omega_{\rm E}^{-1/2}\xi_{n_\tau,n_\kappa}^{m_\tau,m_\kappa}\right)^2}{2}\right)\right]\\ &=\log_2 MN_t-I_1^J-I_2^J.\end{aligned} \tag{42}$$

The second term at the RHS of (42), I_1^J, can be simplified as

$$I_1^J=\frac{1}{MN_t}\sum_{m_\tau=1}^{M}\sum_{n_\tau=1}^{N_t}\mathbb{E}_{\tilde{w}_{\rm E}}\left[\log_2\exp\left(\frac{\tilde{w}_{\rm E}^2}{2}\right)\right]=\log_2 e\;\mathbb{E}_{\tilde{w}_{\rm E}}\left[\frac{\tilde{w}_{\rm E}^2}{2}\right]=\frac{1}{2}\log_2 e. \tag{43}$$

Due to the concavity of $\log_2(\cdot)$, the third term at the RHS of (42), I_2^J, can be lower bounded by applying the Jensen's inequality as

$$\begin{aligned}I_2^J&\le\frac{1}{MN_t}\sum_{m_\tau=1}^{M}\sum_{n_\tau=1}^{N_t}\log_2\sum_{m_\kappa=1}^{M}\sum_{n_\kappa=1}^{N_t}\mathbb{E}_{\tilde{w}_{\rm E}}\left[\exp\left(-\frac{\left(\tilde{w}_{\rm E}+\Omega_{\rm E}^{-1/2}\xi_{n_\tau,n_\kappa}^{m_\tau,m_\kappa}\right)^2}{2}\right)\right]\\ &=-\frac{1}{2}+\frac{1}{MN_t}\sum_{m_\tau=1}^{M}\sum_{n_\tau=1}^{N_t}\log_2\sum_{m_\kappa=1}^{M}\sum_{n_\kappa=1}^{N_t}\exp\left(-\frac{(\xi_{n_\tau,n_\kappa}^{m_\tau,m_\kappa})^2}{4\Omega_{\rm E}}\right).\end{aligned} \tag{44}$$

Finally, upon substituting (43) and (44) into (42), we can obtain

$$\mathbb{I}^J(S,\mathbf{h}_{\rm E};Z)\ge\log_2 MN_t-\frac{1}{2}(\log_2 e-1)\\ -\frac{1}{MN_t}\sum_{m_\tau=1}^{M}\sum_{n_\tau=1}^{N_t}\log_2\sum_{m_\kappa=1}^{M}\sum_{n_\kappa=1}^{N_t}\exp\left(-\frac{(\xi_{n_\tau,n_\kappa}^{m_\tau,m_\kappa})^2}{4\Omega_{\rm E}}\right), \tag{45}$$

which completes the proof of Theorem 2. ■

E. Approximation for AMI

Furthermore, based on Theorem 1 and Theorem 2, we below derive the approximate expressions for $\mathbb{I}^J(S, h_{\mathrm{B}}; Y)$ and $\mathbb{I}^J(S, h_{\mathrm{E}}; Z)$, respectively. Firstly, when $\varrho_{\mathrm{B}} \to \infty$ and $\varrho_{\mathrm{B}} \to 0$, we can derive the limits of (31) $\mathbb{I}^J(S, h_{\mathrm{B}}; Y)$, which are

$$\lim_{\varrho_{\mathrm{B}} \to \infty} \mathbb{I}^J(S, h_{\mathrm{B}}; Y) = \log_2 MN_t, \qquad \lim_{\varrho_{\mathrm{B}} \to 0} \mathbb{I}^J(S, h_{\mathrm{B}}; Y) = 0. \tag{46}$$

Secondly, from (40), we can obtain the limits of $\mathbb{I}_L^J(S, h_{\mathrm{B}}; Y)$ for $\varrho_{\mathrm{B}} \to \infty$ and $\varrho_{\mathrm{B}} \to 0$ as

$$\lim_{\varrho_{\mathrm{B}} \to \infty} \mathbb{I}_L^J(S, h_{\mathrm{B}}; Y) = \log_2 MN_t - \frac{1}{2}(\log_2 e - 1), \tag{47}$$

$$\lim_{\varrho_{\mathrm{B}} \to 0} \mathbb{I}_L^J(S, h_{\mathrm{B}}; Y) = -\frac{1}{2}(\log_2 e - 1). \tag{48}$$

When we compare the results in (46) and (47), we can see that there exists a constant gap $\frac{1}{2}(\log_2 e - 1)$ between the AMI and its corresponding lower bound in both high and low SNR regions. Furthermore, it can be shown that both $\mathbb{I}^J(S, h_{\mathrm{B}}; Y)$ and $\mathbb{I}_L^J(S, h_{\mathrm{B}}; Y)$ are monotonically increasing functions w.r.t. ϱ_{B}. From these observations, we can be inferred that for any given SNR, especially for a SNR located in the high or low SNR region, the difference between $\mathbb{I}^J(S, h_{\mathrm{B}}; Y)$ and $\mathbb{I}_L^J(S, h_{\mathrm{B}}; Y)$ should approximately be a constant of $\frac{1}{2}(\log_2 e - 1)$. With similar argument, we can know that the difference between $\mathbb{I}^J(S, h_{\mathrm{E}}; Z)$ and $\mathbb{I}_L^J(S, h_{\mathrm{E}}; Z)$ is also approximately a constant of $\frac{1}{2}(\log_2 e - 1)$.

Therefore, we may conclude that $\mathbb{I}^J(S, h_{\mathrm{B}}; Y)$ can be closely approximated as

$$\mathbb{I}^J(S, h_{\mathrm{B}}; Y) \approx \mathbb{I}_L^J(S, h_{\mathrm{B}}; Y) + \frac{1}{2}(\log_2 e - 1), \tag{49}$$

and from Theorem 2, we have

$$\mathbb{I}_A^J(S, h_{\mathrm{B}}; Y) \approx \log_2 MN_t - \frac{1}{MN_t} \sum_{m_\tau=1}^{M} \sum_{n_\tau=1}^{N_t} \log_2 \sum_{m_\kappa=1}^{M} \sum_{n_\kappa=1}^{N_t} \exp\left(-\frac{\left(\zeta_{n_\tau, n_\kappa}^{m_\tau, m_\kappa}\right)^2}{4\sigma_{\mathrm{B}}^2} \right). \tag{50}$$

Similarly, we have

$$\mathbb{I}_A^J(S, h_{\mathrm{E}}; Z) \approx \log_2 MN_t - \frac{1}{MN_t} \sum_{m_\tau=1}^{M} \sum_{n_\tau=1}^{N_t} \log_2 \sum_{m_\kappa=1}^{M} \sum_{n_\kappa=1}^{N_t} \exp\left(-\frac{\left(\zeta_{n_\tau, n_\kappa}^{m_\tau, m_\kappa}\right)^2}{4\Omega_{\mathrm{E}}} \right). \tag{51}$$

Consequently, by subtracting the approximation of the AMI between Alice and Eve $\mathbb{I}_A^J(S, h_{\mathrm{E}}; Z)$ from that of $\mathbb{I}_A^J(S, h_{\mathrm{B}}; Y)$ between Alice and Bob, the approximately achievable secrecy rate

of Bob in our SM-VLC system with optical jamming can be expressed as

$$\begin{aligned} R_{A,\text{sec}}^{J} &= \left[\mathbb{I}_A^J(S,h_{\text{B}};Y) - \mathbb{I}_A^J(S,h_{\text{E}};Z)\right]^+ \\ &= \left[\frac{1}{MN_t}\sum_{m_\tau=1}^{M}\sum_{n_\tau=1}^{N_t}\log_2\left[\frac{\sum_{m_\kappa=1}^{M}\sum_{n_\kappa=1}^{N_t}\exp\left(-\frac{\left(\xi_{n_\tau,n_\kappa}^{m_\tau,m_\kappa}\right)^2}{4\Omega_{\text{E}}}\right)}{\sum_{m_\kappa=1}^{M}\sum_{n_\kappa=1}^{N_t}\exp\left(-\frac{\left(\zeta_{n_\tau,n_\kappa}^{m_\tau,m_\kappa}\right)^2}{4\sigma_{\text{B}}^2}\right)}\right]\right]^+ \\ &= \frac{1}{MN_t}(\Upsilon_2-\Upsilon_1), \end{aligned} \tag{52}$$

where, by definition, $\Upsilon_1 = \sum_{m_\tau=1}^{M}\sum_{n_\tau=1}^{N_t}\log_2\sum_{m_\kappa=1}^{M}\sum_{n_\kappa=1}^{N_t}\exp\left(-\frac{(\zeta_{n_\tau,n_\kappa}^{m_\tau,m_\kappa})^2}{4\sigma_{\text{B}}^2}\right)$, and $\Upsilon_2 = \sum_{m_\tau=1}^{M}\sum_{n_\tau=1}^{N_t}\log_2\sum_{m_\kappa=1}^{M}\sum_{n_\kappa=1}^{N_t}\exp\left(-\frac{(\xi_{n_\tau,n_\kappa}^{m_\tau,m_\kappa})^2}{4\Omega_{\text{E}}}\right)$.

F. Error Performance Analysis

In our considered optical jamming assisted SM-VLC system, the task of the detectors employed by Bob and Eve are to determine which data symbol and LED index is selected by the transmitter during a symbol period, i.e., to decide which channel is activated for delivering information, and the utilized data symbol intensity should also be decoded. Since the LED index and data symbol are equiprobably selected, the optimal detector employed by Bob can be designed by following the criterion of maximum likelihood (ML) detection, expressed as

$$[\hat{n}_{\text{B},t},\hat{s}_m] = \underset{n_t\in\{1,\cdots,N_t\},s_m\in\mathcal{S}}{\arg\min}\ |y-h_{\text{B},n_t}s_m|^2. \tag{53}$$

Correspondingly, the optimal detector employed by Eve can be represented as

$$[\hat{n}_{\text{E},t},\hat{s}_m] = \underset{n_t\in\{1,\cdots,N_t\},s_m\in\mathcal{S}}{\arg\min}\ |\tilde{z}-\tilde{h}_{\text{E},n_t}s_m|^2. \tag{54}$$

Below, we analyze the error performance of Bob and Eve employing the detectors of (53) and (54). To begin with, let us derive the pairwise error probability (PEP) of the detection at Bob, $\text{P}(h_{\text{B},n_t}s_\mu \mapsto h_{\text{B},n_\tau}s_\nu|\mathbf{h}_{\text{B}},S)$, which denotes the probability of detecting the symbol s_ν transmitted from the n_τ-th LED, while instead the n_t-th LED is actually activated and transmits symbol s_μ, and it can be expressed as

$$\text{P}(h_{\text{B},n_t}s_\mu \mapsto h_{\text{B},n_\tau}s_\nu|\mathbf{h}_{\text{B}},S) = \text{P}\left(|y-h_{\text{B},n_t}s_\mu|^2 > |y-h_{\text{B},n_\tau}s_\nu|^2\right) = \mathcal{Q}\left(\frac{|\zeta_{n_t,n_\tau}^{m_\mu,m_\nu}|}{2\sigma_{\text{B}}}\right). \tag{55}$$

where $\mathcal{Q}(\cdot)$ is the Gaussian $\mathcal{Q}$-function, and is defined as $\mathcal{Q}(x) = \frac{1}{\sqrt{2\pi}}\int_x^\infty \exp\left(-\frac{t^2}{2}\right)dt$. Note that, the last equation holds, since $2\zeta_{n_t,n_\tau}^{m_\mu,m_\nu}w_{\text{B}}$ is a random variable following the Gaussian distribution of $2\zeta_{n_t,n_\tau}^{m_\mu,m_\nu}w_{\text{B}} \sim \mathcal{N}(0,4(\zeta_{n_t,n_\tau}^{m_\mu,m_\nu})^2\sigma_{\text{B}}^2)$.

Consequently, with the aid of the union-bound approach [38], we can express the upper-bound BER at Bob as

$$\begin{aligned}\mathrm{P}_{\mathrm{B,bit}} &\leq \frac{1}{mMN_t}\sum_{n_t=1}^{N_t}\sum_{m_\mu=1}^{M}\sum_{n_\tau=1}^{N_t}\sum_{m_\nu=1}^{M} H_d\left(h_{\mathrm{B},n_t}s_\mu \mapsto h_{\mathrm{B},n_\tau}s_\nu\right)\mathrm{P}(h_{\mathrm{B},n_t}s_\mu \mapsto h_{\mathrm{B},n_\tau}s_\nu|\mathbf{h}_\mathrm{B},S)\\ &= \frac{1}{mMN_t}\sum_{n_t=1}^{N_t}\sum_{m_\mu=1}^{M}\sum_{n_\tau=1}^{N_t}\sum_{m_\nu=1}^{M} H_d\left(h_{\mathrm{B},n_t}s_\mu \mapsto h_{\mathrm{B},n_\tau}s_\nu\right)\mathcal{Q}\left(\frac{|\zeta_{n_t,n_\tau}^{m_\mu,m_\nu}|}{2\sigma_\mathrm{B}}\right). \end{aligned} \tag{56}$$

where $H_d\left(h_{\mathrm{B},n_t}s_\mu \mapsto h_{\mathrm{B},n_\tau}s_\nu\right)$ is the Hamming distance between the bits representations of $h_{\mathrm{B},n_t}s_\mu$ and $h_{\mathrm{B},n_\tau}s_\nu$. Similarly, the upper-bounded BER of Eve is expressed as

$$\mathrm{P}_{\mathrm{E,bit}} \leq \frac{1}{mMN_t}\sum_{n_t=1}^{N_t}\sum_{m_\mu=1}^{M}\sum_{n_\tau=1}^{N_t}\sum_{m_\nu=1}^{M} H_d\left(h_{\mathrm{E},n_t}s_\mu \mapsto h_{\mathrm{E},n_\tau}s_\nu\right)\mathcal{Q}\left(\frac{|\zeta_{n_t,n_\tau}^{m_\mu,m_\nu}|}{2\Omega_\mathrm{E}^{\frac{1}{2}}}\right). \tag{57}$$

In order to further simplify the computation, we may exploit the tight upper bound for the $\mathcal{Q}$ function [39], which is given by $\mathcal{Q}(x) \leq \sum_{n=1}^{3} a_n \exp(-b_n x^2)$, where $a_1 = \frac{1}{6}, a_2 = \frac{1}{12}, a_3 = \frac{1}{4}$, $b_1 = 2, b_2 = 1, b_3 = \frac{1}{2}$. As a result, the PEP of the detection at Bob can be expressed as

$$\begin{aligned}\mathrm{P}(h_{\mathrm{B},n_t}s_\mu \mapsto h_{\mathrm{B},n_\tau}s_\nu|\mathbf{h}_\mathrm{B},S) \leq{}& \frac{1}{6}\exp\left(-\frac{(\zeta_{n_t,n_\tau}^{m_\mu,m_\nu})^2}{2\sigma_\mathrm{B}^2}\right)\\ &+\frac{1}{12}\exp\left(-\frac{(\zeta_{n_t,n_\tau}^{m_\mu,m_\nu})^2}{4\sigma_\mathrm{B}^2}\right)+\frac{1}{4}\exp\left(-\frac{(\zeta_{n_t,n_\tau}^{m_\mu,m_\nu})^2}{8\sigma_\mathrm{B}^2}\right). \end{aligned} \tag{58}$$

IV. Power Allocation Strategy

In practical applications, when we have some a priori location distribution information about Eve, a secrecy enhancement strategy can be designed to achieve best secrecy performance of the considered SM-VLC system. Specifically, an optimal power allocation between confidential information bearing signal and optical jamming signal exists. As we discussed in section III, the average power constraint of the confidential signal can be represented as $\mathcal{P}_1 = s^2$. As for the optical jamming signal with certain constraints σ_J and A_2, the average power constraint $\mathcal{P}_2$ can be expressed as

$$\begin{aligned}\mathcal{P}_2 &= (N_t-1)\left[1-\frac{\frac{2A_2^*}{\sigma^*}f\left(\frac{A_2^*}{\sigma^*}\right)}{2\Phi\left(\frac{A_2^*}{\sigma^*}\right)-1}\right]\sigma^{*2}\\ &= \left[1-\frac{\frac{2A_2^*}{\sigma^*}f\left(\frac{A_2^*}{\sigma^*}\right)}{2\Phi\left(\frac{A_2^*}{\sigma^*}\right)-1}\right]\sigma_J^2\\ &\triangleq g(A_2), \end{aligned} \tag{59}$$

where f and Φ are defined as in Section III, $\sigma^{*2} = \frac{\sigma_J^2}{N_t-1}$ and $A_2^* = \frac{A_2}{N_t-1}$. Hence, the total power per transmission can be denoted as $\mathcal{P} = \mathcal{P}_1 + \mathcal{P}_2$. Then, $\mathcal{P}$ can be further expressed as

$$\mathcal{P} = \mathcal{P}_1 + \mathcal{P}_2 = s^2 + g(A_2) \leq s^2 + \sigma_J^2. \tag{60}$$

Observe from (60) that, for the considered SM-VLC system, the required total maximum power per transmission is $s^2 + \sigma_J^2$. As a result, if the power shared to the confidential information-bearing signal is $s^2 = \kappa\mathcal{P}$, then the associated power of optical jamming signal expresses as $\sigma_J^2 = (1-\kappa)\mathcal{P}$, where κ is the power allocation factor.

As for the considered power allocation strategy of SM-VLC system, we suppose that Alice has all the channel information $h_{\mathbf{B},n_t}$ and $h_{\mathbf{E},n_t}$ of Bob and Eve. According to these information, Alice can adapt the value of power allocation factor κ to achieve the optimal achievable secrecy rate of the system considered. Hence, the considered power allocation strategy is referred to as the adaptive power allocation approach. Except for the cost of relatively high computation complexity, the optimal value set of κ for achieving the highest secrecy rate at different SNRs can be obtained by a one-dimensional search algorithm, which is accomplished by computing the closed-form secrecy rate expressions of (52).

V. Simulation and Numerical Results

In this section, to validate the analytical secrecy performance and demonstrate the efficiency of the proposed optical jamming secrecy enhancement strategy, we provide numerical results in an indoor VLC environment with the dimensions of $5 \times 5 \times 3$ m^3, which is explained by a three-dimensional (3D) Cartesian coordinate system (O_X, O_Y, O_Z) with the origin being one corner of the room. The transmit LEDs are assumed to be perpendicular to the ceiling and down-facing to the floor. Similarly, the receivers (Bob and Eve) are located on the desks with the height of 0.85 m from the floor, which are assumed to be perpendicular to the desk and up-facing the ceiling. Unless specially noted, we assume that the positions of LEDs are those presented in Table I.

The half-illuminance semi-angle of LED $\Phi_{1/2}$ is set to be $60°$, which is a typical value for commercially-available high-brightness LEDs [4]. Both Bob and Eve have a $60°$ FoV (semi-angle), the area of each PD is $A_{\text{PD}} = 1.0$ cm^2 and the responsivity is $R = 100$ **μA/mW** [4]. For convenience, all the parameters involved in simulations are summarized in Table II.

TABLE I

THE DISTRIBUTIONS OF THE LEDS' LOCATIONS

4 LEDs		8 LEDs	
LED	(O_X, O_Y, O_Z)	1	$(1.25, 0.625, 3.0)$ m
1	$(1.25, 1.25, 3.0)$ m	2	$(3.75, 0.625, 3.0)$ m
2	$(3.75, 1.25, 3.0)$ m	3	$(1.25, 1.875, 3.0)$ m
3	$(1.25, 3.75, 3.0)$ m	4	$(3.75, 1.875, 3.0)$ m
4	$(3.75, 3.75, 3.0)$ m	5	$(1.25, 3.125, 3.0)$ m
		6	$(3.75, 3.125, 3.0)$ m
		7	$(1.25, 4.375, 3.0)$ m
		8	$(3.75, 4.375, 3.0)$ m

TABLE II

SIMULATION PARAMETERS

Simulation setup	
Room size $(L \times W \times H)$	$5 \times 5 \times 3$ m^3
Number of LEDs	$2, 4, 8$
LEDs (D) height	3 m
Receivers (Bob and Eve) height	0.85 m
Transmitter parameters	
Semi-angle at half power ($\Phi_{1/2}$)	60°
Optical power/ electric conversion efficiency (η)	813.6 μW/mA
Modulation index (α)	0.1
Receiver parameters	
Refractive index (β)	1.5
Physical area of a PD (A_{PD})	1.0 cm^2
Receiver FoV semi-angle (Ψ_{FoV})	60°
PD responsivity (R)	100 μA/mW

A. Secrecy Performance Comparison of Different Input Distributions

In order to demonstrate the secrecy enhancement efficiency of the finite discrete input distribution compared with continuous uniform input distribution [4] and truncated Gaussian input distribution [18], we consider the following scenario, where Bob is at a fixed position $(2.10; 0.80; 0.85)$ **m and displays the achievable secrecy rate as a function of Eve's location. We assume that** $\kappa = 0.5$**, i.e., the power allocated to the information signal and jamming signals is equal. Other parameters relevant to Bob are shown in Table II. For all three cases, the jamming signals are assumed to obey truncate Gaussian distribution and their variances are determined by** κ**. From the results shown in Fig. 4, all these three methods are able to degrade Eve's reception and the secrecy**

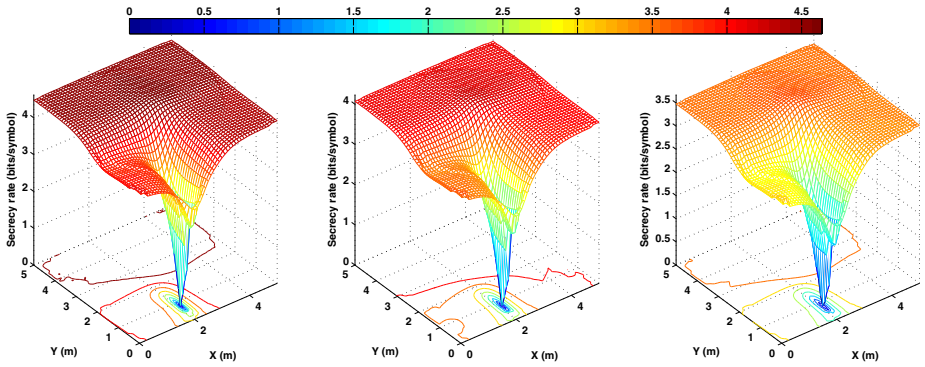

Fig. 4. **Secrecy rate achieved by the VLC system with optical jamming. The left figure depicts the achievable secrecy rate with finite discrete distributed input confidential signals. The middle figure shows the achievable secrecy rate with truncate Gaussian input confidential signals with $\mathcal{TN}(0, 1, -0.2, 0.2)$. The right figure describes the achievable secrecy rate with continuous uniform distributed input signals in the interval $[-1, 1]$.**

rate achieves its maximal value when the location of Eve is far from Bob's location. Additionally, the achievable secrecy rate of the VLC system approaches zero in all three scenarios, when Eve is close to Bob. Furthermore, it can be observed from Fig. 4 that finite discrete inputs provide a better secrecy rate performance compared with continuous uniform input distribution [4] and truncated Gaussian input distribution [18].

B. Secrecy Performance of the SM-VLC Systems Considered

To investigate the secrecy performance of the proposed optical jamming aided secrecy-enhancing scheme, a typical VLC scenario is considered, where we assume that Bob locates at $(2.1516, 1.2768, 0.85)$ m. Unless specially noted, we assume that the power allocated to the information signal and jamming signals is equal, i.e., $\kappa = 0.5$. Other parameters relevant to Bob are shown in Table II.

Fig. 5 depicts the AMI between Alice and Eve from (32) and its lower bound from (41) for the SM-VLC systems operating both with and without optical jamming, where $N_t = 4, 8$ and $M = 4, 8$. Eve is located at $(2.60, 0.88, 0.85)$ m, all other parameters involved in this simulation are taken from Table I and Table II. Observe from the simulation results that upon increasing the SNR, both $\mathbb{I}(S, \mathbf{h}_{\mathrm{E}}; Z)$ and $\mathbb{I}_L(S, \mathbf{h}_{\mathrm{E}}; Z)$ tend to constant values. Moreover, $\mathbb{I}(S, \mathbf{h}_{\mathrm{E}}; Z)$ and $\mathbb{I}_L(S, \mathbf{h}_{\mathrm{E}}; Z)$ also increase, as the number of LEDs N_t and that of the activated LEDs n_t is increased. Furthermore, the gap between $\mathbb{I}(S, \mathbf{h}_{\mathrm{E}}; Z)$ and $\mathbb{I}_L(S, \mathbf{h}_{\mathrm{E}}; Z)$ in the low- and high-SNR regions is approximately a constant of $\frac{1}{2}(\log_2 e - 1)$, which coincides with the theoretical analysis. **It should be noted that when we have $N_t = 8$, the gap between**

$\mathbb{I}^J(S, h_{\mathbf{E}}; Z)$ and $\mathbb{I}_L^J(S, h_{\mathbf{E}}; Z)$ in the high-SNR region is slightly higher than $\frac{1}{2}(log_2 e - 1)$, and there is an error less than 1% averaged over 100 simulations (it is about 0.6%), which is imposed by the approximation error of using $\mathcal{N}(0, 1)$ to estimate the distribution of $\tilde{w}_{\mathbf{E}}$. However, for $N_t \geq 10$, this error can be gradually eliminated. For example, for $N_t = 12$, the error is less than 0.1% averaged over 100 simulations (it is about 0.07%), and $N_t = 20$, the error is less than 10^{-5} averaged over 100 simulations. Additionally, Fig. 5 reveals that the proposed optical jamming strategy is capable of dramatically decreasing the AMI between Alice and Eve for all the cases considered. In particular, for the scenario associated with $N_t = 4, M = 8$, when SNR = 40 dB, the AMI between Alice and Eve is $\mathbb{I}(S, \mathbf{h}_{\mathrm{E}}; Z) = 4.98$ bits/symbol. After applying optical jamming, we have $\mathbb{I}(S, \mathbf{h}_{\mathrm{E}}; Z) = 1.02$ bits/symbol, which is reduced substantially. Hence, all the proposed SM-VLC systems are capable of achieving an improved secrecy performance, when employing the optical jamming advocated.

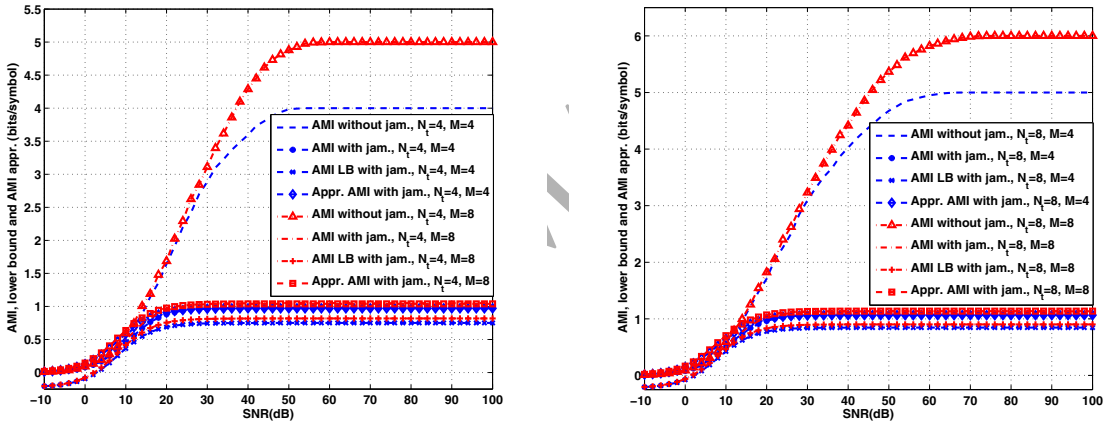

(a) (b)

Fig. 5. AMI between Alice and Eve as well as its lower bound performance (a) $N_t = 4, M = 4, 8$ and (b) $N_t = 8, M = 4, 8$ in the SM-VLC systems with and without optical jamming. The results were calculated from (32) and (41).

Fig. 6 characterizes both the AMI between Alice and Bob from (31) as well as that between Alice and Eve from (32) in Section III-C. The achievable secrecy rate of the VLC systems operating with and without optical jamming calculated from (52) is also shown in Fig. 6, where we have $N_t = 4, 8, M = 4, 8$, Bob's position is fixed at $(2.16, 1.28, 0.85)$ m and Eve is located at $(2.60, 0.88, 0.85)$ m. All other parameters involved in this simulation are taken from Table I and Table II. It is seen that in all the four cases, the achievable secrecy rate increases as the SNR increases, which is the explicit benefit of optical jamming.

Fig. 7 demonstrates the achievable secrecy rate of the SM-VLC system from (52) with

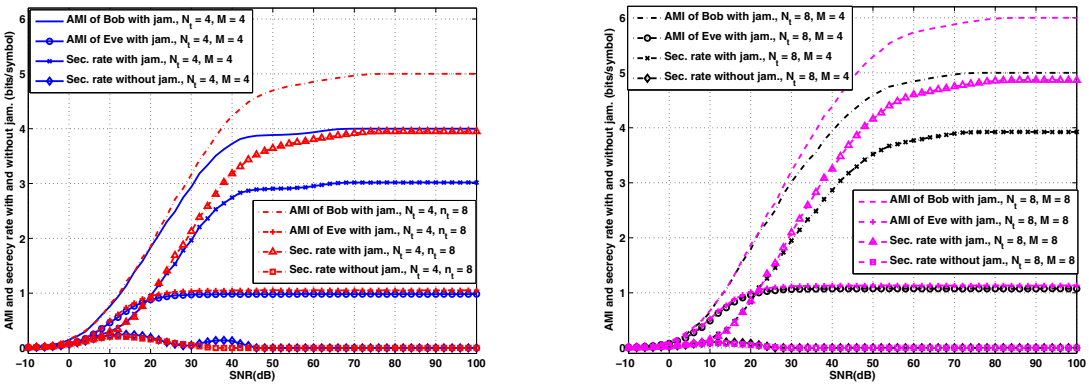

(a) (b)

Fig. 6. AMI between S and D as well as that between Alice and Eve, and achievable secrecy rate performance (a) $N_t = 4, M = 4, 8$ in the SM-VLC and (b) $N_t = 8, M = 4, 8$ in the SM-VLC systems with and without optical jamming. The results were calculated from (31), (32) and (52).

optical jamming, where (a) $N_t = 4, M = 4$; (b) $N_t = 4, M = 8$; (c) $N_t = 8, M = 4$ and (d) $N_t = 8, M = 8$. Eve's location is varied across the 2D plane at a height of 0.85 m, while Bob's position is fixed at $(2.15, 1.28, 0.85)$ m, all other parameters involved in this simulation are taken from Table I and Table II. The SNR is 40 dB for Fig. 7. Observe from Fig. 7 that the secrecy rate of the SM-VLC system approaches zero for all four cases, when Bob is close to Eve.

In Fig. 8, the achievable secrecy rate of the SM-VLC system from (52) is depicted for the cases, where $N_t = 4, 8, M = 4, 8$, and Bob's location is varied, while that of Eve is fixed at the location of $(2.90, 0.88, 0.85)$ m. All other parameters involved in this simulation are taken from Table I and Table II. It can be observed from Fig. 8 that in most of the area considered, the SM-VLC system achieves a relatively stable secrecy rate. The main reason behind this is that even for high SNRs, the detection performance of Eve can still be degraded by optical jamming, without affecting the reception performance of Bob, since the jamming signals are designed to lie in the null space of $\mathbf{h}_{\mathrm{B},n_t}$. As expected, when Eve moves close to Bob, the achievable secrecy rate is significantly reduced. However, the achievable secrecy rate of the SM-VLC system increases rapidly, as Eve moves away from Bob. Additionally, when Eve is located at the symmetric regions of the projection of the transmitters, the achievable secrecy rate increases, which confirms the analytical results of [26]. Furthermore, we can also infer from the results of Fig. 8 that the achievable secrecy rate of the SM-VLC system has a relatively high correlation with Bob's location. When Eve's location is fixed, again there are symmetric regions exhibiting a low achievable secrecy rate.

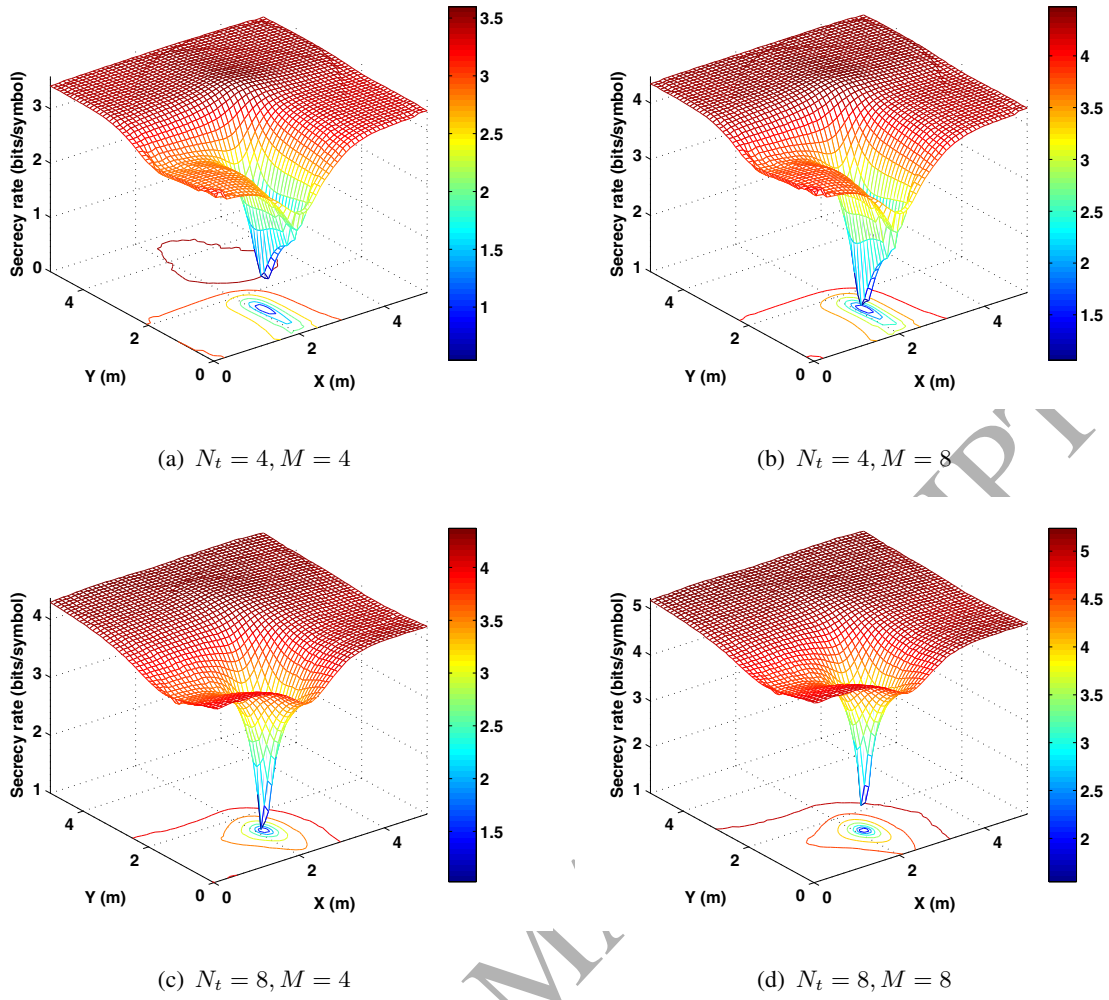

(a) $N_t = 4, M = 4$

(b) $N_t = 4, M = 8$

(c) $N_t = 8, M = 4$

(d) $N_t = 8, M = 8$

Fig. 7. Secrecy rate achieved by the SM-VLC system with optical jamming, where (a) $N_t = 4, M = 4$; (b) $N_t = 4, M = 8$; (c) $N_t = 8, M = 4$ and (d) $N_t = 8, M = 8$, SNR = 40 dB, Bob's location is fixed, whereas Eve's location is varied. The results were calculated from (52).

C. Trade-off between the BER and the Secrecy Performance

In this subsection, we show the variations of the secrecy performance of the SM-VLC system considered with different allocations of the power sharing factors κ.

Fig. 9 shows the BER performance of Alice for the SM-VLC systems relying on optical jamming and different power sharing factors κ, where Eve is located at $(2.60, 0.88, 0.85)$ m. Observe from the simulation results that the BER performance of Eve is dramatically degraded due to the optical jamming. We also see that when the portion of power allocated to the jamming signal exceeds a threshold, such as 0.5 in the high-SNR region, the reduction of κ appears to have a negligible impact on the BER performance of Eve. However, the BER performance of Bob is heavily degraded when more power is allocated to optical jamming, which can be observed in the Fig. 10.

Explicitly, Fig. 10 characterizes the impact of the power sharing factor κ on the BER

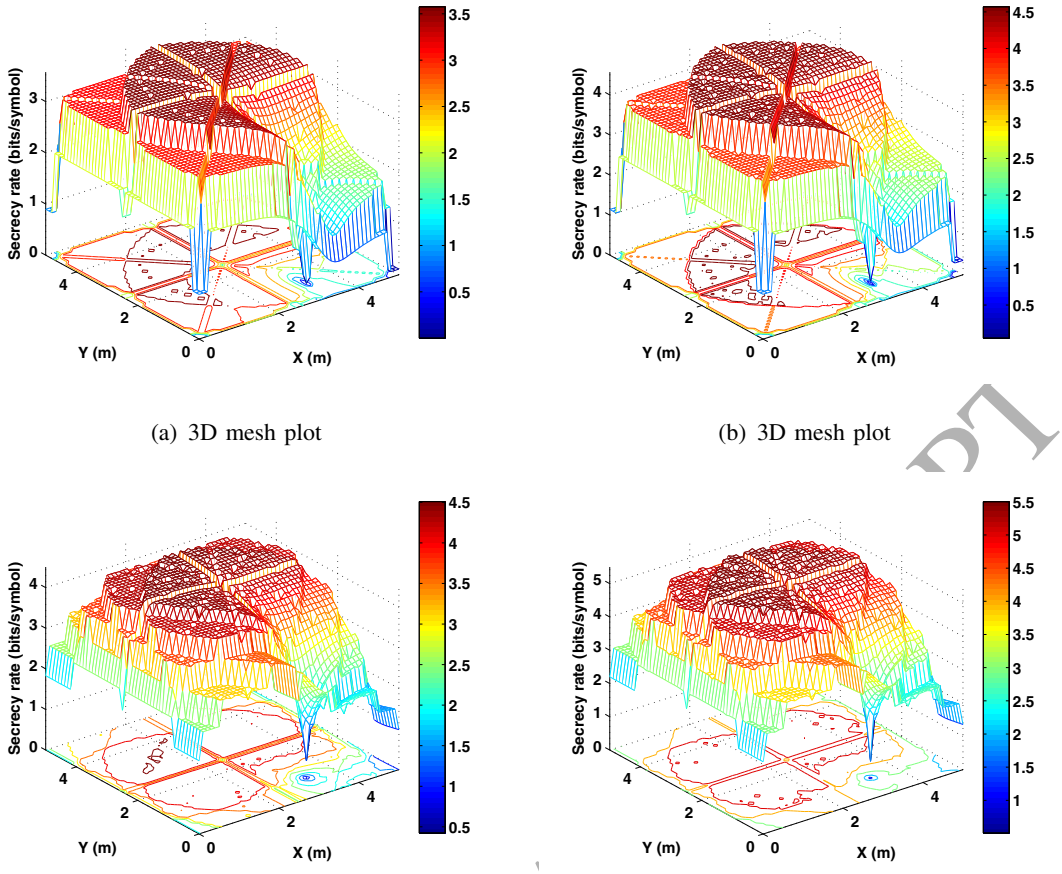

(a) 3D mesh plot (b) 3D mesh plot

(c) 3D mesh plot (d) 3D mesh plot

Fig. 8. Secrecy rate achieved by the SM-VLC system with optical jamming, where (a) $N_t = 4, M = 4$; (b) $N_t = 4, M = 8$; (c) $N_t = 8, M = 4$ and (d) $N_t = 8, M = 8$, SNR = 40 dB, Eve's location is fixed, whereas Bob's location is varied. The result

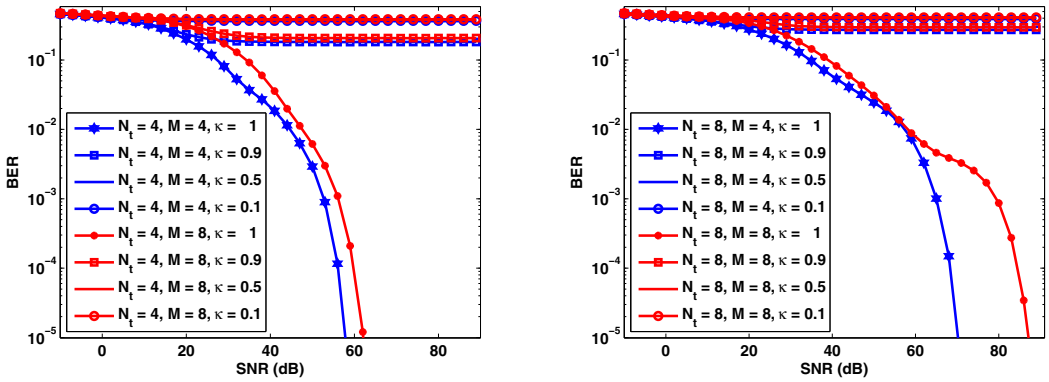

(a) (b)

Fig. 9. BER performance of Eve with $\kappa = 0.1$, 0.5, 0.9 and 1 for different systems. (a) $N_t = 4, 4, M = 4, 8$; (b) $N_t = 8, M = 4, 8$. All other parameters involved in this simulation are taken from Table I and Table II.

performance of the Alice to Bob link, where we have $N_t = 4, 8, M = 4, 8$, Bob is located at $(2.15, 1.28, 0.85)$ m and we depict the BER versus SNR performance results of Bob by letting $\kappa = 0.1 : 0.1 : 1$, respectively, all other parameters involved in this simulation are taken from Table I and Table II. Using the same settings as in Fig. 10, we demonstrate the

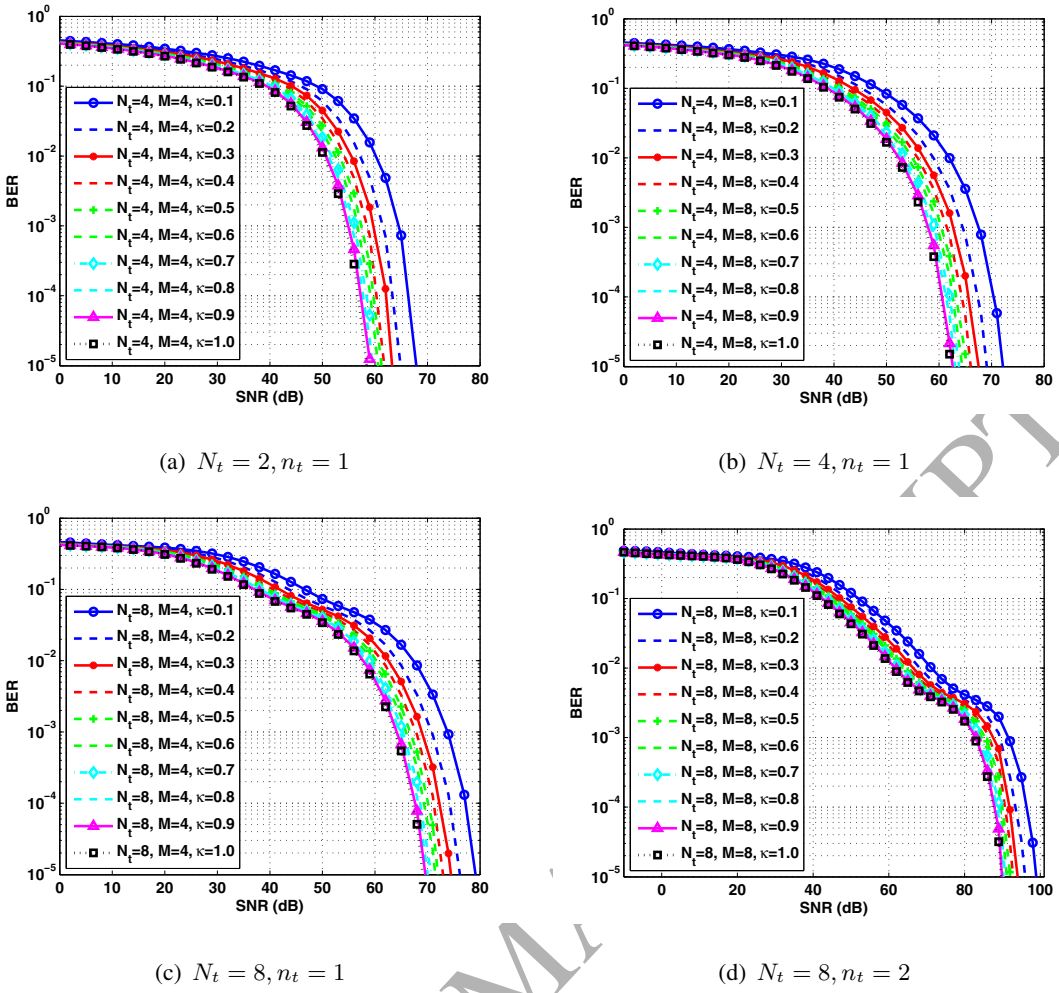

(a) $N_t = 2, n_t = 1$ (b) $N_t = 4, n_t = 1$

(c) $N_t = 8, n_t = 1$ (d) $N_t = 8, n_t = 2$

Fig. 10. BER performance of Alice to Bob link vs. κ of our SM-VLC systems. (a) $N_t = 4, M = 4$; (b) $N_t = 4, M = 8$; (c) $N_t = 8, M = 4$; (d) $N_t = 8, M = 8$.

impact of the power sharing factor κ on the achievable secrecy rate of the systems as well, which are shown in Fig. 11. We can readily find from Fig. 10 that the BER performance of Bob is affected by the power sharing schemes. Furthermore, the BER performance of Bob can be enhanced, when a higher percentage of power is assigned to it. However, even if more power is allocated to Bob, relying on $\kappa \geq 0.5$, the BER performance improvement of Bob remains modest for the SM-VLC systems investigated, while the achievable secrecy rate is dramatically decreased as demonstrated in Fig. 11. Hence, how to determine the optimal power sharing factor for striking a trade-off between the hypothetical by achievable secrecy rate and the desired BER performance becomes critical for practical applications.

From the results shown in Fig. 10 and 11, we can observe that for all the considered four SM-VLC systems operating in the high-SNR region, when $\kappa = 1$, we get the best BER performance, while the achievable secrecy rate approaches its minimum. By contrast, when $\kappa = 0.1$, the BER performance becomes the worst within the SNR range considered and the system attains the best secrecy performance. We observe furthermore that, 1) For the

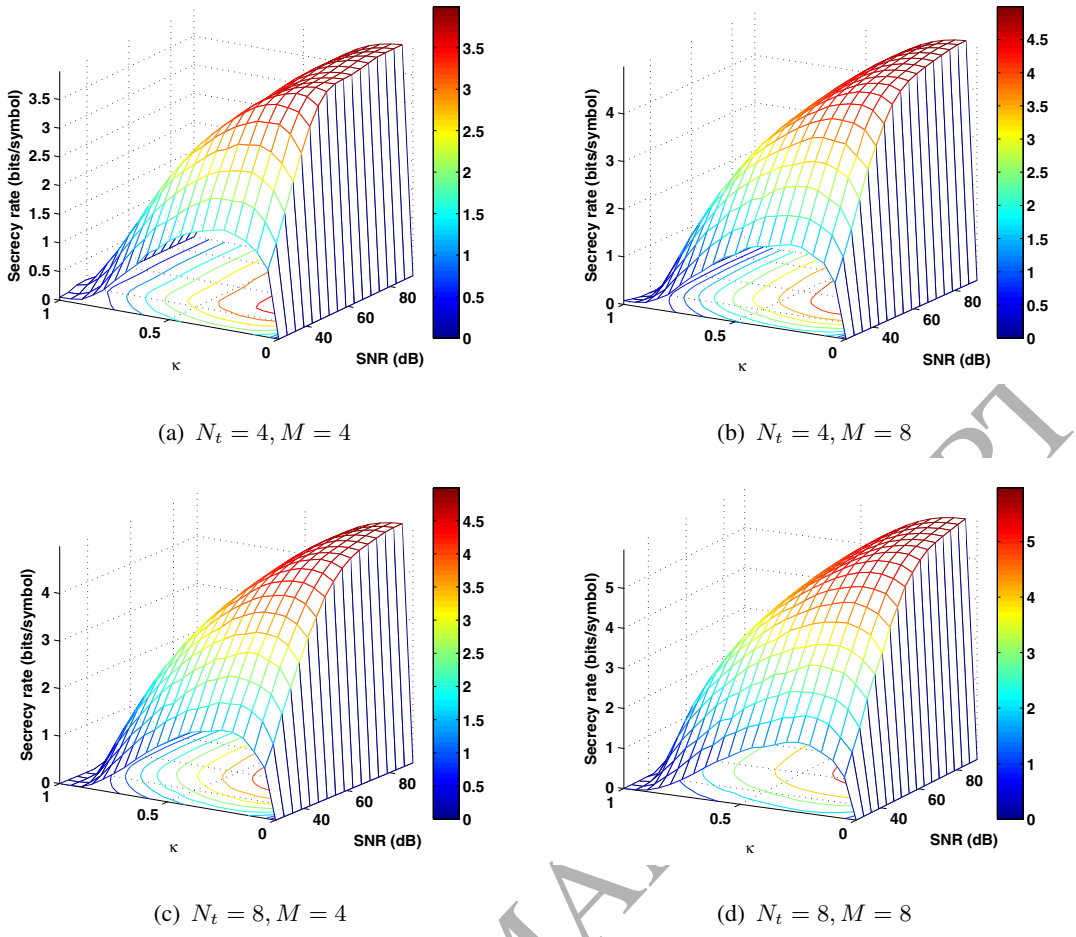

(a) $N_t = 4, M = 4$ (b) $N_t = 4, M = 8$

(c) $N_t = 8, M = 4$ (d) $N_t = 8, M = 8$

Fig. 11. Secrecy performance of the SM-VLC systems considered vs κ and SNR. (a) $N_t = 4, M = 4$; (b) $N_t = 4, M = 8$; (c) $N_t = 8, M = 4$; (d) $N_t = 8, M = 8$. **The results were calculated from** (52).

SM-VLC system associated with $N_t = 4, M = 4$, when κ varies from 1 to 0.5, the SNR degradation at a BER of 10^{-5} is about 1.5 dB, whereas the achievable secrecy rate can be increased by 2 bit/symbol; 2) For the SM-VLC system having $N_t = 4, M = 8$, when κ varies from 1 to 0.5, the SNR degradation at a BER of 10^{-5} is about 2.5 dB, whereas the achievable secrecy rate can be increased by 3.8 bits/symbol; 3) For the SM-VLC system having $N_t = 8, M = 4$, when κ varies from 1 to 0.5, the SNR degradation at a BER of 10^{-5} is about 2.5 dB, whereas the achievable secrecy rate can be increased by 3.7 bits/symbol; 4) For the SM-VLC system using $N_t = 8, M = 8$, when κ varies from 1 to 0.5, the SNR degradation at a BER of 10^{-5} is about 1.8 dB, whereas the achievable secrecy rate can be increased by 5.1 bits/symbol.

From Fig. 10 and 11, we can conclude that the achievable secrecy rate increases, as more power is assigned to the jamming signals, *i.e.* for smaller κ. However, when a low power is allocated to the confidential information signal, the BER of the Alice to Bob link is degraded, especially when κ is less than 0.5. The trade-off between the secrecy performance and the BER performance should be carefully considered for each application. Based on our analysis,

a look-up table can be constructed to guide the system design of the optical jamming aided SM-VLC systems, so that the system parameters can be optimal by selected for the system considered. If the system is secrecy-critical, we may opt for a relatively low power sharing factor κ. Otherwise, if the BER performance is the most important metric of the system considered, then more power should be allocated to the information signals. For the SM-VLC systems jointly considering the secrecy and BER performance, based on the above results, we can opt for a power sharing factor of $\kappa = 0.5$ in the relatively high-SNR region and $\kappa = 1$ in the lower-SNR region.

VI. Conclusions

In this paper, A PLS technique aided secrecy performance analysis and enhancement approach for SM-VLC system was investigated. Accordingly, four major contributions have been proposed: Firstly, by exploiting the characteristic of the input signals and channels of the proposed SM-VLC system, the secrecy performance is analyzed when the input signals are assumed to have finite discrete distributions with amplitude and power constraints. From these results, we conclude that, without extra secrecy enhancement strategy, Eve can easily wiretap the confidential signals at high SNR even if its channel condition is worse than Bob. Moreover, if the Alice-to-Bob channel is degraded, the system cannot provide secrecy communication. Secondly, a friendly optical jamming aided secrecy enhancement scheme for the proposed SM-VLC system is designed. Apart from transmitting optical jamming signals by the exist LEDs, Alice sends simultaneously the confidential signal along these LEDs with appropriate amplitude and power constraints. Wherein, we adopt the truncated Gaussian distribution for optical jamming signals to satisfy these constraints. Furthermore, the optical jamming signals are generated from the nullspace of the Alice-to-Bob channel vector. Thirdly, the secrecy performance of SM-VLC system with optical jamming is analyzed. Fourthly, the optimal power allocation strategy for the proposed SM-VLC system with optical jamming is considered, which is addressed between confidential information and interference transmission for maximizing the achievable secrecy rate of the proposed system. Specially, A trade-off suggestion on how to select an optimal power sharing factor was provided. Finally, all the analytic results achieved from analysis have been verified by comprehensive computer simulations.

References

[1] H. Elgala, R. Mesleh, and H. Haas, "Indoor optical wireless communication: Potential and state-of-the-art," *IEEE Commun. Mag.*, vol. 49, no. 9, pp. 56–62, Sep. 2011.

[2] D. Karunatilaka, F. Zafar, V. Kalavally, and R. Parthiban, "LED based indoor visible light communications: State of the art," *IEEE Commun. Surveys Tuts.*, vol. 17, no. 3, pp. 1649–1678, 2015.

[3] R. Zhang, H. Claussen, H. Haas, and L. Hanzo, "Energy efficient visible light communications relying on amorphous cells," *IEEE J. Sel. Areas Commun.*, vol. 34, no. 4, pp. 894–906, Apr. 2016.

[4] A. Mostafa and L. Lampe, "Physical-Layer security for MISO visible light communication channels," *IEEE J. Sel. Areas Commun.*, vol. 33, no. 9, pp. 1806–1818, Sep. 2015.

[5] J. Classen, J. Chen, D. Steinmetzer, M. Hollick, and E. Knightly, "The spy next door: Eavesdropping on high throughput visible light communications," in *Proc. ACM VLCS'2015*, Paris, Sep. 2015, pp. 9–14.

[6] J. Classen, D. Steinmetzer, and M. Hollick, "Opportunities and pitfalls in securing visible light communication on the physical layer," in *Proc. ACM VLCS'2016*, New York, Oct. 2016, pp. 19–24.

[7] Y. S. Shiu, S. Y. Chang, H. C. Wu, S. C. H. Huang, and H. H. Chen, "Physical layer security in wireless networks: A tutorial," *IEEE Wireless Commun.*, vol. 18, no. 2, pp. 66–74, Apr. 2011.

[8] Y.-W. P. Hong, P.-C. Lan, and C.-C. J. Kuo, *Signal Processing Approaches to Secure Physical Layer Communications in Multi-Antenna Wireless Systems*. New York, NY, USA: Springer-Verlag, 2014.

[9] Y. Zou, J. Zhu, X. Wang, and L. Hanzo, "A survey on wireless security: Technical challenges, recent advances, and future trends," *Proc. IEEE*, vol. 104, no. 9, pp. 1727–1765, Sep. 2016.

[10] X. Chen, D. W. K. Ng, W. Gerstacker, and H. H. Chen, "A survey on multiple-antenna techniques for physical layer security," *IEEE Commun. Surveys Tuts.*, vol. 19, no. 2, pp. 1027–1053, 2016.

[11] Y. Liu, H. H. Chen, and L. Wang, "Physical layer security for next generation wireless networks: Theories, technologies, and challenges," *IEEE Commun. Surveys Tuts.*, vol. 19, no. 1, pp. 347–376, 2017.

[12] S. R. Aghdam and T. M. Duman, "Joint precoder and artificial noise design for MIMO wiretap channels with finite-alphabet inputs based on the cut-off rate," *IEEE Trans. Wireless Commun.*, vol. 16, no. 6, pp. 3913–3923, Jun. 2017.

[13] A. Lapidoth, S. M. Moser, and M. A. Wigger, "On the capacity of free-space optical intensity channels," *IEEE Trans. Inf. Theory*, vol. 55, no. 10, pp. 4449–4461, Oct. 2009.

[14] A. Chaaban, J. M. Morvan, and M. S. Alouini, "Free-space optical communications: Capacity bounds, approximations, and a new sphere-packing perspective," *IEEE Trans. Commun.*, vol. 64, no. 3, pp. 1176–1191, Mar. 2016.

[15] R. Jiang, Z. Wang, Q. Wang, and L. Dai, "A tight upper bound on channel capacity for visible light communications," *IEEE Commun. Lett.*, vol. 20, no. 1, pp. 97–100, Jan. 2016.

[16] A. Chaaban, Z. Rezki, and M. S. Alouini, "Fundamental limits of parallel optical wireless channels: Capacity results and outage formulation," *IEEE Trans. Commun.*, vol. 65, no. 1, pp. 296–311, Jan. 2017.

[17] A. Mostafa and L. Lampe, "Securing visible light communications via friendly jamming," in *Proc. IEEE GLOBECOM Wkshps'2014*, Dec. 2014, pp. 524–529.

[18] H. Zaid, Z. Rezki, A. Chaaban, and M. S. Alouini, "Improved achievable secrecy rate of visible light communication with cooperative jamming," in *Proc. IEEE GLOBALSIP'2015*, Dec. 2015, pp. 1165–1169.

[19] S. Ma, Z. L. Dong, H. Li, Z. Lu, and S. Li, "Optimal and robust secure beamformer for indoor MISO visible light communication," *J. Lightw. Technol.*, vol. 34, no. 21, pp. 4988–4998, Nov. 2016.

[20] A. Mostafa and L. Lampe, "Optimal and robust beamforming for secure transmission in MISO visible-light communication links," *IEEE Trans. Signal Process.*, vol. 64, no. 24, pp. 6501–6516, Dec. 2016.

[21] S. Goel and R. Negi, "Guaranteeing secrecy using artificial noise," *IEEE Trans. Wireless Commun.*, vol. 7, no. 6, pp. 2180–2189, Jun. 2008.

[22] H. Shen, Y. Deng, W. Xu, and C. Zhao, "Secrecy-oriented transmitter optimization for visible light communication systems," *IEEE Photo. J.*, vol. 8, no. 5, pp. 1–14, Oct. 2016.

[23] F. I. K. Mousa, N. A. Maadeed, K. Busawon, A. Bouridane, and R. Binns, "Secure MIMO visible light communication system based on user's location and encryption," *J. Lightw. Technol.*, vol. 35, no. 24, pp. 5324–5334, Dec. 2017.

[24] G. Pan, J. Ye, and Z. Ding, "On secure VLC systems with spatially random terminals," *IEEE Commun. Lett.*, vol. 21, no. 3, pp. 492–495, Mar. 2017.

[25] ——, "Secure hybrid VLC-RF systems with light energy harvesting," *IEEE Trans. Commun.*, vol. 65, no. 10, pp. 4348–4359, Oct. 2017.

[26] F. Wang, C. Liu, Q. Wang, J. Zhang, R. Zhang, L. L. Yang, and L. Hanzo, "Secrecy analysis of generalized space-shift keying aided visible light communication," *IEEE Access*, vol. 6, pp. 18 310–18 324, 2018.

[27] R. Mesleh, H. Elgala, and H. Haas, "Optical spatial modulation," *IEEE/OSA J. Optical Commun. Netw.*, vol. 3, no. 3, pp. 234–244, Mar. 2011.

[28] X. Wang, X. Wang, and L. Sun, "Spatial modulation aided physical layer security enhancement for fading wiretap channels," in *2016 8th International Conference on Wireless Communications Signal Processing (WCSP)*, Oct 2016, pp. 1–5.

[29] E. Curry and D. K. Borah, "Iterative combinatorial symbol design for spatial modulations in MIMO VLC systems," *IEEE Photonic. Tech. L.*, vol. 30, no. 5, pp. 483–486, March 2018.

[30] J. M. Kahn and J. R. Barry, "Wireless infrared communications," *Proc. IEEE*, vol. 85, no. 2, pp. 265–298, Feb. 1997.

[31] L. Zeng, D. C. O'Brien, H. L. Minh, G. E. Faulkner, K. Lee, D. Jung, Y. Oh, and E. T. Won, "High data rate multiple input multiple output (MIMO) optical wireless communications using white LED lighting," *IEEE J. Sel. Areas Commun.*, vol. 27, no. 9, pp. 1654–1662, Dec. 2009.

[32] T. Fath, H. Haas, M. D. Renzo, and R. Mesleh, "Spatial modulation applied to optical wireless communications in indoor los environments," in *2011 IEEE Global Telecommunications Conference - GLOBECOM 2011*, Dec 2011, pp. 1–5.

[33] R. A. Horn and C. R. Johnson, *Matrix Analysis*, 2nd ed. New York, NY, USA: Cambridge University Press, 2012.

[34] Z. I. Botev, "The normal law under linear restrictions: Simulation and estimation via minimax tilting," *J. Royal Stat. Soc.: Ser. B-Stat. Methodol.*, vol. 79, no. 1, pp. 125–148, Jan. 2017.

[35] C. M. Jarque and A. K. Bera, "A test for normality of observations and regression residuals," *International Statistical Review/Revue Internationale de Statistique*, pp. 163–172, 1987.

[36] R. G. Gallager, *Information theory and reliable communication*. Hoboken, NJ, USA: Wiley, 1968.

[37] T. M. Cover and J. A. Thomas, *Elements of Information Theory*. Hoboken, NJ, USA: Wiley, 2006.

[38] J. G. Proakis and M. Salehi, *Digital communications*. New York, NY, USA: McGraw-Hill, 2008.

[39] M. Chiani, D. Dardari, and M. K. Simon, "New exponential bounds and approximations for the computation of error probability in fading channels," *IEEE Trans. Wireless Commun.*, vol. 2, no. 4, pp. 840–845, Jul. 2003.